2011

NEW ENERGY EXPRESSIONS FOR MODEL KOHN-SHAM POTENTIALS

Pavel D. Elkind

NEW ENERGY EXPRESSIONS FOR MODEL KOHN–SHAM POTENTIALS

(Thesis format: Monograph)

by

Pavel D. Elkind

Graduate Program in Chemistry

A thesis submitted in partial fulfillment
of the requirements for the degree of
Master of Science

The School of Graduate and Postdoctoral Studies
The University of Western Ontario
London, Ontario, Canada

THE UNIVERSITY OF WESTERN ONTARIO
School of Graduate and Postdoctoral Studies

CERTIFICATE OF EXAMINATION

Department Examiners:

Dr. David M. Wardlaw

Supervisor:

Dr. Styliani Constas

Dr. Viktor N. Staroverov

University Examiner:

Dr. Colin Denniston

The thesis by

Pavel D. Elkind

entitled:

New Energy Expressions for Model Kohn–Sham Potentials

is accepted in partial fulfillment of the
requirements for the degree of
Master of Science

Date

/ Dr. David W. Shoesmith
Chair of the Thesis Examination Board

Abstract

In the Kohn–Sham density-functional theory, one has to approximate ("model") either the exchange-correlation density functional or the corresponding exchange-correlation potential. If one chooses to approximate the potential, then one needs to use the van Leeuwen–Baerends line integral to assign an energy to the density coming from a given approximate potential. The problem with this approach is that when a model potential does not have a parent functional, the line integral is path-dependent and so the energy is ambiguously defined. For such potentials, existing paths are far from optimal. In this work, we introduce two new density parametrizations for the line-integral formula and obtain the corresponding energy expressions. We then use these expressions to explore several existing model exchange potentials. The first energy expression corresponds to a path in which the electron density is constructed by gradually filling *frozen* Kohn–Sham orbitals in accordance with the aufbau principle, either orbital-by-orbital or subshell-by-subshell. The second energy expression uses the Janak theorem and requires knowing the dependence of the highest-occupied molecular orbital (HOMO) energy on the HOMO's occupation number. We also propose a new derivation of Janak's theorem that reveals its connection to the van Leeuwen–Baerends line integral. In addition, we revisit Slater's transition-state method and show that in the intervals between N and $N-1$ electrons, the total energy calculated from a typical density-functional approximation deviates from linearity quadratically. We also find that the HOMO energy calculated for an $(N-1/2)$-electron system becomes almost exact, which indicates that the $(N-1/2)$-electron potential is more accurate than the potential of the N-electron system. This suggests that the accuracy of molecular properties calculated with existing approximate exchange-correlation functionals may be improved if the corresponding Kohn–Sham potentials are constructed from electron-deficient densities.

Keywords: quantum chemistry, density-functional theory, density-functional approximations, exchange-correlation potential, fractionally charged systems.

Acknowledgments

The author wishes to thank Professor Viktor N. Staroverov for the warmest hospitality in his research group and for the enormous amount of time he devoted to the author's development. The author also wishes to thank his current and former group fellows Brian D. Nikkel, Mohammadamin Torabi, Alex P. Gaiduk and especially Dr. Ilya G. Ryabinkin for countless fruitful discussions and for the friendly atmosphere they all maintained.

Contents

List of Figures

List of Tables

1 Introduction

Nonrelativistic quantum-mechanical treatment of an N-electron system is based on the electronic Schrödinger equation. This equation is a partial differential equation of $3N$ spatial and N spin variables. Solving the Schrödinger equation analytically even for two-electron systems is an intractable problem, so one has to resort either to numerical grid methods or to approximation techniques. Numerical grids are computationally too expensive except for small systems. There exist many *ab initio* approximation methods that allow for systematic improvement and, in principle, for arbitrary accuracy, but they also become prohibitively expensive in applications to large systems. A possible way to overcome this problem is to use density-functional theory (DFT). DFT is in principle assured to deliver the same electron density and the same ground-state energy as the exact solution of the Schrödinger equation. In addition, DFT naturally allows one to treat systems of thousands of particles, which makes it the most widely-used computation approach in present-day quantum chemistry and solid-state physics.

1.1 Hohenberg–Kohn density-functional theory

The Hamiltonian operator $\hat{H}$ for an interacting system of M nuclei and N electrons, considered in vacuum, at 0 K, in the absence of any external fields, can be written as

$$\hat{H} = \hat{T} + \hat{V}_{\mathrm{ee}} + \hat{V}, \tag{1.1}$$

where the first term is the operator for the kinetic energy of the electrons (we use atomic units throughout the text)

$$\hat{T} = -\frac{1}{2}\sum_{i=1}^{N} \nabla_i^2, \tag{1.2}$$

the second term is the operator which describes the electron-electron repulsion energy

$$\hat{V}_{\text{ee}} = \sum_{i<j}^{N} \frac{1}{|\mathbf{r}_i - \mathbf{r}_j|}, \tag{1.3}$$

and the last term is the operator for the energy of the electron-nuclear attraction

$$\hat{V} = \sum_{i=1}^{N} v(\mathbf{r}_i), \tag{1.4}$$

in which

$$v(\mathbf{r}) = -\sum_{A=1}^{M} \frac{Z_A}{|\mathbf{r} - \mathbf{R}_A|} \tag{1.5}$$

is the external Coulomb potential due to the nuclei. In the above equations, $\mathbf{r}_i$ denotes the spatial coordinates of the i-th electron; $\mathbf{R}_A$ and Z_A denote the spatial coordinates and the charge of the A-th nucleus. The above Hamiltonian does not contain the term describing the kinetic energy of the nuclei since the Born–Oppenheimer approximation has already been applied. Also, for fixed nuclei, the Hamiltonian does not include the term describing the nuclear repulsion energy as it is just a constant vertical shift of the total energy, specific to the system under study. In addition, the Hamiltonian does not contain electron spins, which effectively makes it nonrelativistic.

Let us analyze the Hamiltonian of Eq. (1.1). The operators for the kinetic energy $\hat{T}$ and the electron-electron repulsion energy $\hat{V}_{\text{ee}}$ are the same for every system. This implies that all system-specific information, apart from the number of electrons, is encoded in the external potential $v(\mathbf{r})$. This suggests that the total energy of the system can be thought of as a functional of the external potential

$$E = \langle \Psi | \hat{H} | \Psi \rangle = E[v]. \tag{1.6}$$

In 1964, Hohenberg and Kohn proved an important theorem [1] stating that the electron density ρ uniquely determines the external potential v. For instance, in the

case of non-degenerate ground states, there is a one-to-one correspondence between ρ and v: $\rho \leftrightarrow v$. In the case of degenerate ground states, the relationship is many-to-one: $\rho \rightarrow v$. Since the density uniquely determines the external potential, $\rho \rightarrow v$, and since the external potential uniquely determines the ground-state energy, $v \rightarrow E[v]$, one can think of the total energy as a functional of the electron density, $E[\rho]$.

According to Hohenberg and Kohn, the total-energy density functional $E[\rho]$ is written as

$$E[\rho] = F[\rho] + \int \rho(\mathbf{r}) v(\mathbf{r})\, d\mathbf{r}, \tag{1.7}$$

where $F[\rho]$ is the *universal* density functional. For systems with non-degenerate ground states, the existence of the universal density functional is best demonstrated by the constrained-search argument due to Levy [2]:

$$F[\rho] = \min_{\Psi \rightarrow \rho} \langle \Psi | \hat{T} + \hat{V}_{\mathrm{ee}} | \Psi \rangle. \tag{1.8}$$

Here the minimization is done over all possible N-particle antisymmetric wavefunctions Ψ that correspond to the given density ρ. In the case of degenerate systems, the search domain in Eq. (1.8) is extended to ensembles of antisymmetric N-electron wavefunctions. We will discuss ensembles in greater detail in Sections 3 and 4.

The density functional $F[\rho]$ is called universal because it is *system-independent* in the sense that it is the same for every system containing some particular number of electrons. The system-independence of the universal density functional comes from the fact that it describes only those contributions to the total energy that come from system-independent operators $\hat{T}$ and $\hat{V}_{\mathrm{ee}}$.

Hohenberg and Kohn also demonstrated that the total-energy density functional $E[\rho]$ of Eq. (1.7) is variational, that is, for any N-representable trial density ρ it gives

an energy which is above the exact ground-state electron energy E_0:

$$E[\rho] \geq E_0. \tag{1.9}$$

This fact allows one to obtain (or to approximate) the exact ground-state electron density by minimizing the total-energy functional with respect to the density. The term N-representable means any density that comes from an N-electron antisymmetric wavefunction Ψ. For a density to be N-representable, it has to (i) be non-negative everywhere, (ii) integrate to N, and (iii) satisfy the following condition [1, 3]:

$$\int |\nabla \rho^{1/2}(\mathbf{r})|^2 \, d\mathbf{r} < \infty, \tag{1.10}$$

which comes from the restriction that the kinetic energy, $\langle \Psi | \hat{T} | \Psi \rangle$, has to be finite. Only densities that satisfy the above requirements may be used in the definition of the universal density functional $F[\rho]$ and, therefore, only these densities may be used in the variational minimization of the total-energy density functional. In practice, the N-representability condition is satisfied for any reasonable density. The density functional $E[\rho]$, however, is unknown, which poses an interesting challenge of constructing practical approximations to it. The Kohn–Sham method is a possible way to proceed with this.

1.2 Kohn–Sham method

Although the Hohenberg–Kohn theorem ensures the existence of the universal density functional, it does not suggest a way of constructing it. In 1965, a year after Hohenberg and Kohn had published their work, Kohn and Sham found a way to "carry this approach further" [4].

To introduce the Kohn–Sham method, let us consider a fictitious system of non-interacting electrons moving in some external potential v_s. For this system, the exact

analytic solution of the Schrödinger equation is known—it is a single-determinantal wavefunction built from one-electron wavefunctions (orbitals). Orbitals φ_i are solutions of the following one-particle Schrödinger-like equation:

$$\left(-\frac{1}{2}\nabla^2 + v_s\right)\varphi_i = \epsilon_i \varphi_i. \tag{1.11}$$

Orbitals may or may not include spin coordinates. In principle, the Hamiltonian $\hat{H}$ of Eq. (1.1) does not depend on spin, so spin coordinates are not necessary. However, it is much easier to enforce the Pauli antisymmetry constraint on the wavefunction by using spins. For this reason, it is customary to include spin in the form of "spin-orbitals", which are products of spatial orbitals $\varphi_i(\mathbf{r})$ and one-electron spin functions α or β.

The total energy of non-interacting electrons, therefore, can be written as

$$E[\rho] = T_s[\rho] + \int \rho(\mathbf{r})\, v_s(\mathbf{r})\, d\mathbf{r}, \tag{1.12}$$

where $T_s[\rho]$ is the total kinetic energy of N non-interacting electrons:

$$T_s[\rho] = -\frac{1}{2}\sum_{i=1}^{N}\langle\varphi_i|\nabla^2|\varphi_i\rangle. \tag{1.13}$$

The electron density in this case is simply

$$\rho(\mathbf{r}) = \sum_{i=1}^{N}|\varphi_i(\mathbf{r})|^2. \tag{1.14}$$

The expression in Eq. (1.12) is exact for non-interacting electrons. By comparing it with Eq. (1.7), we see that the universal density functional $F[\rho]$ in the case of non-interacting electrons is equal to $T_s[\rho]$. This result suggests using $T_s[\rho]$ as a part of the true universal density functional $F[\rho]$ for *interacting* electrons. That is what Kohn

and Sham proposed. Specifically, they split the true universal density functional in the following way:

$$F[\rho] = T_s[\rho] + J[\rho] + E_{\rm xc}[\rho], \tag{1.15}$$

where

$$J[\rho] = \frac{1}{2}\int\int d\mathbf{r}\, d\mathbf{r}'\, \frac{\rho(\mathbf{r})\rho(\mathbf{r}')}{|\mathbf{r}-\mathbf{r}'|} \tag{1.16}$$

is the energy of the Coulomb self-repulsion of the electron density ρ, and $E_{\rm xc}[\rho]$ is the *exchange-correlation functional.* This functional is defined by Eq. (1.15) as that part of $F[\rho]$ which must be added to $T_s[\rho] + J[\rho]$ to yield $F[\rho]$.

In view of Eq. (1.15), the total-energy density functional for interacting electrons becomes

$$E[\rho] = T_s[\rho] + J[\rho] + E_{\rm xc}[\rho] + \int \rho(\mathbf{r})v(\mathbf{r})\, d\mathbf{r}. \tag{1.17}$$

Kohn and Sham assumed that the density minimizing the above functional can be simultaneously the density of non-interacting electrons moving in some external potential. So the idea is to find such an external potential v_s that would describe the real interacting system. Then this potential is used in equations for non-interacting electrons [Eq. (1.11)] to obtain the Kohn–Sham orbitals and, consequently, the density of the interacting system. By comparing Euler–Lagrange equations for the total-energy functional of non-interacting electrons [Eq. (1.12)] and for the total-energy functional of interacting electrons [Eq. (1.17)], Kohn and Sham concluded that

$$v_s(\mathbf{r}) = v_J(\mathbf{r}) + v(\mathbf{r}) + v_{\rm xc}(\mathbf{r}), \tag{1.18}$$

where

$$v_J(\mathbf{r}) \equiv \frac{\delta J[\rho]}{\delta\rho(\mathbf{r})} = \int d\mathbf{r}'\, \frac{\rho(\mathbf{r}')}{|\mathbf{r}-\mathbf{r}'|} \tag{1.19}$$

is the electrostatic potential due to the electron density, $v(\mathbf{r})$ is the potential due to

the nuclei [Eq. (1.5)], and

$$v_{\mathrm{xc}}(\mathbf{r}) \equiv \frac{\delta E_{\mathrm{xc}}[\rho]}{\delta \rho(\mathbf{r})} \tag{1.20}$$

is the *exchange-correlation potential.* The electrostatic potential of the density $v_J(\mathbf{r})$ and the exchange-correlation potential $v_{\mathrm{xc}}(\mathbf{r})$ are formally defined as functional derivatives of the corresponding functionals (see Section 1.3).

After substituting the external potential v_s corresponding to the real physical system [Eq. (1.18)] into the equation for non-interacting electrons [Eq. (1.11)], one obtains the Kohn–Sham equations that describe the physical (interacting) system:

$$\left(-\frac{1}{2}\nabla^2 + v_J + v + v_{\mathrm{xc}}\right)\varphi_i(\mathbf{r}) = \epsilon_i \varphi_i(\mathbf{r}). \tag{1.21}$$

The density constructed by Eq. (1.14) from the orbitals obtained by solving Eq. (1.21) is the density that minimizes the total-energy density functional of interacting electrons [Eq. (1.17)]. The potentials v_J and v_{xc} depend on the density, so the Kohn–Sham equations must be solved self-consistently. The self-consistent procedure consists of the following steps: one starts from an initial guess for the density, then calculates v_J and v_{xc}, finds the Kohn–Sham orbitals φ_i, and finally obtains a new density ρ; these steps are repeated until the density stops changing.

In the original Hohenberg–Kohn formulation, the electron density is required to be N-representable. In the Kohn–Sham scheme, the set of densities is restricted to those that can be constructed only from orbitals that are the solutions of the Kohn–Sham equations [Eq. (1.11)]. Such densities are called v-representable. The class of N-representable densities is wider than the class of v-representable densities, which means that the minimization process in the Kohn–Sham scheme cannot access all possible densities that occur in the Levy constrained search. This is a limitation of the Kohn–Sham scheme. Other than that, the Kohn–Sham method is in principle exact.

As good as it is, the Kohn–Sham scheme requires approximations for the exchange-correlation functional $E_{\rm xc}[\rho]$. Unfortunately, there is no rigorous way of improving existing approximations and introducing new ones. As a result, the Kohn–Sham density-functional theory remains in practice a semi-empirical method, although justified by strong physical arguments.

1.3 Functionals and functional derivatives

Rigorous mathematical treatment of functional derivatives is beyond the scope of this thesis. However, here we will try to give the reader a good feeling of what functionals and functional derivatives are by comparing them to some familiar concepts from calculus.

A function is a prescription of how to assign a *number* to another *number*. A functional is a generalization of the concept of a function. Specifically, a functional is a rule of assigning a *number* to a *function*. An example of a functional is the value of a definite integral,

$$F[f] = \int_a^b f(x)\,dx. \tag{1.22}$$

Here $F[f]$ is the number that corresponds to the function f. One of the simplest functionals which one may encounter in density-functional theory is the exchange-energy density functional for a uniform electron gas:

$$E_{\rm x}^{\rm LDA}[\rho] = -C_{\rm x}\int \rho^{4/3}(\mathbf{r})\,d\mathbf{r}, \tag{1.23}$$

where $C_{\rm x} = \frac{3}{4}\left(\frac{3}{\pi}\right)^{1/3}$. This functional is also known as the local density approximation (LDA) to the exact exchange-correlation functional. The integration in Eq. (1.23) is over the entire three-dimensional space of the spatial coordinate $\mathbf{r}$.

A very common problem in calculus is to find an extremum of a function. This is

usually done by searching for stationary points, i.e., those points where the derivative of the function vanishes. An extremum, if any, may be achieved only at the stationary points or at the boundaries of the function's domain.

In the calculus of variations, there exists a similar problem of finding a function that delivers an extremum value of a functional. In this context, the concept of a *functional derivative* arises. For a given density $\rho(\mathbf{r})$ and an arbitrary integrable function $h(\mathbf{r})$, consider the functional

$$DF[\rho, h] = \lim_{\tau \to 0} \frac{F[\rho + \tau h] - F[\rho]}{\tau} = \tag{1.24}$$

$$= \left\{ \frac{d}{d\tau} F[\rho + \tau h] \right\}_{\tau=0}. \tag{1.25}$$

If the limit in Eq. (1.24) exists, i.e., if the above functional exists, and if $DF[\rho, h]$ is linear in h, then it is usually possible to bring it into the following form:

$$DF[\rho, h] = \int v(\mathbf{r}) h(\mathbf{r})\, d\mathbf{r}, \tag{1.26}$$

where $v(\mathbf{r}) \equiv \dfrac{\delta F[\rho]}{\delta \rho(\mathbf{r})}$ *defines* the functional derivative of a given functional $F[\rho]$.

In practice, in order to find a functional derivative, one evaluates the variation $DF[\rho, h]$ by using Eqs. (1.24) or (1.25), converts the result into the form of Eq. (1.26), and then deduces the functional derivative $v(\mathbf{r})$.

As an example, let us evaluate the functional derivative of the LDA exchange functional $E_{\mathrm{x}}^{\mathrm{LDA}}[\rho]$. Using Eq. (1.25) we obtain:

$$\begin{aligned} DE_{\mathrm{x}}^{\mathrm{LDA}}[\rho] &= -C_{\mathrm{x}} \left\{ \frac{d}{d\tau} \int (\rho + \tau h)^{4/3}\, d\mathbf{r} \right\}_{\tau=0} \\ &= -C_{\mathrm{x}} \left\{ \int \frac{4}{3} (\rho + \tau h)^{1/3}\, h\, d\mathbf{r} \right\}_{\tau=0} \\ &= -C_{\mathrm{x}} \int \frac{4}{3} \rho^{1/3}\, h\, d\mathbf{r}, \end{aligned} \tag{1.27}$$

from which we conclude, by comparison with Eq. (1.26), that the functional derivative of the LDA functional is

$$v_{\mathrm{x}}^{\mathrm{LDA}}(\mathbf{r}) \equiv \frac{\delta E_{\mathrm{x}}^{\mathrm{LDA}}[\rho]}{\delta \rho(\mathbf{r})} = -\frac{4}{3} C_{\mathrm{x}} \rho^{1/3}(\mathbf{r}). \tag{1.28}$$

Taking the functional derivative of an approximate exchange-correlation functional results in the corresponding exchange-correlation potential [Eq. (1.20)]. So in the example above, we have derived the exchange potential for the local-density approximation, $v_{\mathrm{x}}^{\mathrm{LDA}}(\mathbf{r})$.

The functional derivative of a given functional is a part of the Euler–Lagrange equation which allows one to find the function that delivers an extremum value to the functional under study. In density-functional theory, the Kohn–Sham equations represent the Euler–Lagrange equation for the total-energy density functional $E[\rho]$ of Eq. (1.17) minimized subject to the constraint that the electron density always integrates to the number of electrons.

As we mentioned before, the local-density functional $E_{\mathrm{x}}^{\mathrm{LDA}}[\rho]$ is one of the simplest possible functionals in density-functional theory. Many other approximate functionals involve not only the electron density but also its derivatives $\nabla\rho$, $\nabla^2\rho$, etc. Using the method described above, one can show [5] that for a density functional of the form

$$F[\rho] = \int f(\rho, \nabla\rho, \nabla^2\rho)\, d\mathbf{r} \tag{1.29}$$

the functional derivative is given by

$$v(\mathbf{r}) \equiv \frac{\delta F}{\delta \rho} = \frac{\partial f}{\partial \rho} - \nabla \cdot \left(\frac{\partial f}{\partial \nabla \rho} \right) + \nabla^2 \left(\frac{\partial f}{\partial \nabla^2 \rho} \right), \tag{1.30}$$

where $\dfrac{\partial f}{\partial \nabla \rho}$ is a shorthand for a vector with three components $\dfrac{\partial f}{\partial \rho'_\alpha}$, in which $\rho'_\alpha \equiv \dfrac{\partial \rho}{\partial \alpha}$ and $\alpha = x, y, z$. We will elaborate on Eq. (1.30) in Section 2.3. For now, let us

introduce another useful technique.

Suppose that the argument ρ of a functional $F[\rho]$ is itself a function of an additional variable, say, the variable t. In this case the functional parametrically depends on t, which we denote by $F(t) \equiv F[\rho_t]$. The question now is how to evaluate the partial derivative of $F[\rho_t]$ with respect to t. It turns out [5] that the common chain rule of differentiation applies to functionals, so the expression for the derivative of $F[\rho_t]$ is given by

$$\frac{\partial F(t)}{\partial t} = \frac{\partial F[\rho_t]}{\partial t} = \int \frac{\delta F[\rho_t]}{\delta \rho_t(\mathbf{r})} \frac{\partial \rho_t(\mathbf{r})}{\partial t} \, d\mathbf{r}. \tag{1.31}$$

We will employ Eq. (1.31) extensively in the following Sections.

2 Energies from model potentials: Aufbau path

2.1 Motivation

As originally proposed by Kohn and Sham, density-functional theory requires approximations for the exchange-correlation functional, $E_{\mathrm{xc}}[\rho]$. Dozens of density-functional approximations have been introduced to date, some of them being quite successful [6]. However, if one looks closer at the Kohn–Sham scheme, it becomes evident that it is not the exchange-correlation *functional* but its functional derivative, the exchange-correlation *potential*, v_{xc}, that plays the main role in DFT. Only the potential is present in the Kohn–Sham equations, and, consequently, it alone determines the electron density $\rho(\mathbf{r})$ through Kohn–Sham orbitals $\varphi_i(\mathbf{r})$. Moreover, the exchange-correlation potential, in contrast to the functional, is defined only up to an arbitrary *constant*, while the exchange-correlation functional, as any functional, is defined up to an arbitrary *function* that integrates over all space to zero. These two facts make the exchange-correlation potential an attractive object to model. More than a dozen model potentials have been introduced to date [7–22].

The benefits of approximating the exchange-correlation potential come with a price. One part of the trade-off is that the energy functional, corresponding to the model potential, is unknown. It means that one has to find a way of assigning an energy to the density coming from a model potential. Another consideration is that the parent functional for an arbitrary model exchange-correlation potential may not exist.

Assume for a while that for a model potential v_{xc} its parent functional $E_{\mathrm{xc}}[\rho]$ exists. If the explicit form of $E_{\mathrm{xc}}[\rho]$ were known, one would just plug a given density ρ into the functional to calculate the energy corresponding to that density:

$$E_{\mathrm{xc}}[\rho] = \int f(\rho, \nabla\rho, \nabla^2\rho, \dots)\, d\mathbf{r}. \tag{2.1}$$

As the functional is not known, some procedure is needed to obtain the energy. Here we mostly follow the original derivation of van Leeuwen and Baerends [23], who, in the context of density-functional theory, rediscovered Volterra's findings [24] on the general theory of functional calculus. The idea is to introduce an additional parameter t into $\rho(\mathbf{r})$ to create a *path* of densities $\rho_t(\mathbf{r})$. In this case the functional $E_{\mathrm{xc}}[\rho_t]$ becomes a function of the variable t:

$$E_{\mathrm{xc}}(t) \equiv E_{\mathrm{xc}}[\rho_t]. \tag{2.2}$$

The derivative of this function is given by the chain rule of differentiation [Eq. (1.31)]:

$$\frac{\partial E_{\mathrm{xc}}(t)}{\partial t} = \int \frac{\delta E_{\mathrm{xc}}[\rho_t]}{\delta \rho_t(\mathbf{r})} \frac{\partial \rho_t}{\partial t}\, d\mathbf{r} = \int v_{\mathrm{xc}}([\rho_t];\mathbf{r}) \frac{\partial \rho_t}{\partial t}\, d\mathbf{r}. \tag{2.3}$$

Integration of the above derivative from $t = a$ to $t = b$ leads to the following energy difference:

$$E_{\mathrm{xc}}[\rho_b] - E_{\mathrm{xc}}[\rho_a] = \int_a^b \frac{\partial E_{\mathrm{xc}}(t)}{\partial t}\, dt = \int_a^b dt \int v_{\mathrm{xc}}([\rho_t];\mathbf{r}) \frac{\partial \rho_t}{\partial t}\, d\mathbf{r}. \tag{2.4}$$

If the density ρ is parametrized in such a way that $\rho_a = 0$ and ρ_b is equal to the density of interest, $\rho_b = \rho$, then the energy difference from Eq. (2.4) reduces to

$$E_{\mathrm{xc}}[\rho] = \int_a^b dt \int v_{\mathrm{xc}}([\rho_t];\mathbf{r}) \frac{\partial \rho_t}{\partial t}\, d\mathbf{r}. \tag{2.5}$$

The last equation allows one to assign an energy to any model potential v_{xc} constructed from a given density ρ without actually knowing the explicit form of the functional $E_{\mathrm{xc}}[\rho]$.

Equation (2.5) is derived under the assumption that the parent functional $E_{\mathrm{xc}}[\rho]$ for the potential v_{xc} actually exists. For any such potential, the energy obtained from this equation does not depend on the particular parametrization of the density used, as long as $\rho_a = 0$ and $\rho_b = \rho$. However, it may happen that the model potential does

not have a parent functional, that is, it is not a functional derivative. In that case, the energy obtained from Eq. (2.5) will generally depend on the particular parametrization of the density.

Let us introduce some new terminology. We will call a model potential *integrable* if its parent functional exists. If a model potential does not have a parent functional, then we will call it *non-integrable* or *stray*. We will also call some particular parametrization of the density a *density integration path* or simply a *path*. Using this terminology we can reformulate the above paragraph: energies obtained using integrable potentials are path-independent, while energies coming from stray potentials depend on the integration path.

A path ρ_t used in Eq. (2.5) must be such that the derivative $\frac{\partial \rho_t}{\partial t}$ exists almost everywhere, so that the integral over t has a definite value. "Almost everywhere" is a mathematical term, which in this context means that the derivative exists either for all values of t or for all values of t except for a countable set of points.

Several density-scaling paths are known in the literature. None of them, however, was initially introduced in the context of line integration. They served for completely different purposes. The path of uniformly scaled densities [23, 25], which has been called the Q-path [26, 27], is defined by

$$\rho_q(\mathbf{r}) = q\rho(\mathbf{r}), \tag{2.6}$$

where $0 \leq q \leq 1$. We use a distinct letter subscript for the scaling parameter in some particular path and reserve t for the general discussion of any path. Another path is the uniform particle-number conserving density scaling, proposed and extensively studied by Levy [28]:

$$\rho_\lambda(\mathbf{r}) = \lambda^3 \rho(\lambda \mathbf{r}). \tag{2.7}$$

This path has been termed the Λ-path ($0 \leq \lambda \leq 1$). Perdew and co-workers [29]

proposed a Thomas–Fermi-inspired path of the following form:

$$\rho_\zeta(\mathbf{r}) = \zeta^2 \rho(\zeta^{1/3}\mathbf{r}), \tag{2.8}$$

which has been referred to as the Z-path [26, 27]. The path of Eq. (2.8) is originally defined for $0 \leq \zeta \leq \infty$, but the term "Z-path" corresponds to the following range of ζ values: $0 \leq \zeta \leq 1$. There are also non-scaling paths. For instance, van Leeuwen and Baerends [23] used the path

$$\rho_t(\mathbf{r}) = t^3 \rho\left(t\mathbf{r} + (1-t)\mathbf{R}\right), \tag{2.9}$$

where $\mathbf{R}$ is an arbitrary vector, to explicitly show that the energy assigned to a non-integrable model potential is path-dependent. As discussed in Ref. [23], the following path was initially implicitly used by Ziegler and Rauk [30] to calculate molecular binding energies:

$$\rho_t = \rho^\Sigma + t(\rho^M - \rho^\Sigma), \quad 0 \leq t \leq 1. \tag{2.10}$$

Here $\rho^M \equiv \rho_1$ denotes the electron density of a diatomic molecule AB and $\rho^\Sigma \equiv \rho_0 = \rho^A + \rho^B$, in which ρ^A and ρ^B denote the densities of isolated atoms A and B. The above path represents how the superimposed density of individual atoms, ρ^Σ, transforms into molecular density, ρ^M, of the molecule AB.

An important result for the Λ-path can be derived for exchange-only potentials. One of the analytical properties of such potentials is that they are homogeneous of degree one with respect to uniform density scaling (Λ-path) [31]:

$$v_x([\rho_\lambda]; \mathbf{r}) = \lambda v_x([\rho]; \lambda\mathbf{r}). \tag{2.11}$$

Equation (2.11) allows the integral over $\lambda = t$ in Eq. (2.5) to be taken analytically,

leading to the following well-known Levy–Perdew virial formula [32, 33]:

$$E_{\mathrm{x}}[\rho] = \int d\mathbf{r}\, v_{\mathrm{x}}([\rho];\mathbf{r})\,[3\rho(\mathbf{r}) + \mathbf{r}\cdot\nabla\rho(\mathbf{r})]\,. \tag{2.12}$$

Some of the aforementioned paths have been used in the context of line integrals. For example, Gaiduk *et al.* [26] derived potentials from some existing approximate density functionals and then reconstructed these functionals by integrating the potentials along the Q-, Λ- and Z-paths. Reconstructions obtained by using different scaling paths differ in their analytic representation but give the same numerical results. The results also coincide with those obtained directly from the functionals. Gaiduk and Staroverov [27] employed the Q-, Λ- and Z-paths to test whether several existing model potentials were integrable or not. Surprisingly, only a few of existing potentials are integrable.

If a potential is integrable, then its reconstructions using different scaling paths are just gauge transformations of the integrand expression for the parent functional [26]. In the case of non-integrable potentials, the reconstruction is generally path-dependent, but a particular combination of the potential and a path can be thought of as a definition of a new density functional. In this regard, a question arises: For a given potential, which density parametrization defines a better model to approximate the exact $E_{\mathrm{xc}}[\rho]$? This problem was partially addressed in Ref. [27], where the authors calculated total energies for a set of atoms and molecules for non-integrable potentials using the Q-, Λ- and Z-paths.

The principal objective of this work is to introduce new density parametrizations and to assess their performance in comparison with other existing paths. The new paths can be combined with literally any model potential, so, in effect, we are introducing a variety of new approximations to the exact exchange-correlation functional.

2.2 Aufbau paths

Let us now introduce two new density parametrizations to be used in the line integral formula, Eq. (2.5). The first parametrization, which we call the *orbital-aufbau path*, is such that the density is filled orbital-by-orbital from the lower-energy Kohn–Sham orbitals. The formal expression for the orbital-aufbau path may be written as:

$$\rho_t(\mathbf{r}) = \sum_{i=1}^{\lfloor t \rfloor} |\varphi_i^\circ(\mathbf{r})|^2 + \{t\}|\varphi_{\lfloor t+1 \rfloor}^\circ(\mathbf{r})|^2. \tag{2.13}$$

Here the scaling parameter t varies from 0 to the total number of electrons, N. Symbols $\lfloor t \rfloor$ and $\{t\}$ denote the integer and fractional parts of t correspondingly. The superscript $^\circ$ indicates that Kohn–Sham orbitals are frozen, that is, calculated once for the N-electron system and then kept fixed. Note that for one-electron systems, the orbital-aufbau path coincides with the Q-path of Eq. (2.6).

If a system has degenerate orbitals, these orbitals can be filled in any order. This leads to non-uniqueness of the orbital-aufbau path for systems with degeneracy. To avoid this ambiguity, we introduce a more general parametrization, which we call the *subshell-aufbau path*. Here the orbitals are filled from the lowest to the highest not one-by-one but subshell-by-subshell. By a subshell we mean any set of degenerate orbitals. In other words, all degenerate orbitals which have the same orbital energy are filled simultaneously. The subshell-aufbau path is unique for systems with degeneracy and it reduces to the orbital-aufbau path for systems with no degeneracy. The formal expression for the subshell-aufbau path is as follows:

$$\rho_t(\mathbf{r}) = \sum_{i=1}^{\lfloor t \rfloor} S_i(\mathbf{r}) + \{t\} S_{\lfloor t+1 \rfloor}(\mathbf{r}), \tag{2.14}$$

where $S_i(\mathbf{r})$ is a sum of squares of degenerate orbitals which form the i-th subshell:

$$S_i(\mathbf{r}) = \sum_{j=1}^{\#\text{ degen. orb.}} |\varphi_j^\circ(\mathbf{r})|^2. \tag{2.15}$$

The parameter t now varies from 0 to the numbers of subshells N_s in the system.

As discussed above, for a density parametrization to be used in the line-integral formula, the following two equalities must hold: $\rho_t(\mathbf{r})|_{t=a} = 0$ and $\rho_t(\mathbf{r})|_{t=b} = \rho(\mathbf{r})$. In addition, the density $\rho_t(\mathbf{r})$ must be continuous in t. While the first two conditions are clearly satisfied by the orbital- and subshell-aufbau paths, the continuity of $\rho_t(\mathbf{r})$ needs to be proven. To do that, it is sufficient to show that the following equalities hold for every a:

$$\lim_{t\to a+} \rho_t = \lim_{t\to a-} \rho_t = \rho_a. \tag{2.16}$$

For non-integer values of a, these equalities certainly hold. Before looking at integer values of a, let us collect some useful properties of the integer-part and fractional-part functions. For an integer number a, the following equalities hold:

$$\lim_{t\to a-} \lfloor t \rfloor = a - 1; \quad \lim_{t\to a+} \lfloor t \rfloor = a; \quad \lim_{t\to a-} \{t\} = 1; \quad \lim_{t\to a+} \{t\} = 0. \tag{2.17}$$

Keeping these properties in mind, one can easily evaluate the limits of Eq. (2.16):

$$\lim_{t\to a-} \rho_t(\mathbf{r}) = \lim_{t\to a-} \sum_{i=1}^{\lfloor t \rfloor} |\varphi_i^\circ(\mathbf{r})|^2 + \lim_{t\to a-} \{t\} |\varphi_{\lfloor t \rfloor+1}^\circ(\mathbf{r})|^2 = \sum_{i=1}^{a} |\varphi_i^\circ(\mathbf{r})|^2 \tag{2.18}$$

and

$$\lim_{t\to a+} \rho_t(\mathbf{r}) = \lim_{t\to a+} \sum_{i=1}^{\lfloor t \rfloor} |\varphi_i^\circ(\mathbf{r})|^2 + \lim_{t\to a+} \{t\} |\varphi_{\lfloor t \rfloor+1}^\circ(\mathbf{r})|^2 = \sum_{i=1}^{a} |\varphi_i^\circ(\mathbf{r})|^2 \tag{2.19}$$

as well as the value of ρ_a itself, by definition:

$$\rho_a(\mathbf{r}) = \sum_{i=1}^{a} |\varphi_i^\circ(\mathbf{r})|^2. \tag{2.20}$$

As shown above, equalities of Eq. (2.16) hold for all values of a, so the orbital-aufbau path is continuous in t. The proof is identical for the subshell-aufbau path—one just needs to replace $\varphi_i(\mathbf{r})$ with $S_i(\mathbf{r})$ in Eqs. (2.18)–(2.20).

Since we have proved that aufbau paths are continuous, we can use them in the line integral formula. To exploit these new paths, it is also necessary to evaluate the partial derivative $\dfrac{\partial \rho_t}{\partial t}$, which we do by definition. For the orbital-aufbau path:

$$\frac{\partial \rho_t}{\partial t} = \lim_{\Delta t \to 0} \frac{\rho_{t+\Delta t} - \rho_t}{\Delta t}\bigg|_{\mathbf{r}=\text{const}} = \begin{cases} \varphi^\circ_{\lfloor t \rfloor + 1}, \text{ if } t \text{ is not an integer} \\ \text{limit does not exist, if } t \text{ is an integer.} \end{cases} \tag{2.21}$$

Similarly, for the subshell-aufbau path:

$$\frac{\partial \rho_t}{\partial t} = \lim_{\Delta t \to 0} \frac{\rho_{t+\Delta t} - \rho_t}{\Delta t}\bigg|_{\mathbf{r}=\text{const}} = \begin{cases} S_{\lfloor t \rfloor + 1}, \text{ if } t \text{ is not an integer} \\ \text{limit does not exist, if } t \text{ is an integer.} \end{cases} \tag{2.22}$$

The set of points where $\dfrac{\partial \rho_t}{\partial t}$ does not exist is countable (i.e., of zero measure), so the value of the integral over t in the line integral formula is not affected. In other words, $\rho_t(\mathbf{r})$ is a continuous function of t with a discontinuous first derivative, which causes no difficulty in practical applications of the aufbau paths.

The final expression for the exchange-correlation energy in the case of orbital-aufbau path is as follows:

$$E_{\text{xc}}[\rho] = \int_0^N dt \int d\mathbf{r}\, v_{\text{xc}}([\rho_t]; \mathbf{r})\, |\varphi^\circ_{\lfloor t+1 \rfloor}(\mathbf{r})|^2. \tag{2.23}$$

For the subshell-aufbau path, we have

$$E_{\mathrm{xc}}[\rho] = \int_0^{N_s} dt \int d\mathbf{r}\, v_{\mathrm{xc}}([\rho_t];\mathbf{r})\, S_{\lfloor t+1 \rfloor}(\mathbf{r}). \tag{2.24}$$

Aufbau paths are not based on density scaling, so they cannot be represented as the density multiplied by some scaling factor. Instead, aufbau paths deal with Kohn–Sham orbitals as building blocks for the electron density. Since aufbau paths operate with orbitals (or subshells) and have discontinuous derivatives, we expected that these paths, when used in conjunction with model potentials, would mimic the behavior of the exact exchange-correlation potential, which itself has discontinuities at integer electron numbers.

Before we proceed to assess the aufbau paths, let us describe the density functionals and model potentials which we study in this work.

2.3 Functionals and potentials of interest

We start by elaborating on the functional differentiation technique introduced in Section 1.3. Many practical density-functional approximations have the form

$$F[\rho] = \int f(\rho, g)\, d\mathbf{r}, \tag{2.25}$$

where g is the norm of the gradient of the density,

$$g \equiv |\nabla\rho| = \left[\left(\frac{\partial\rho}{\partial x}\right)^2 + \left(\frac{\partial\rho}{\partial y}\right)^2 + \left(\frac{\partial\rho}{\partial z}\right)^2\right]^{1/2}. \tag{2.26}$$

For the functional derivative of a functional written in the form of Eq. (2.25), the general expression for the functional derivative [Eq. (1.30)] can be cast as

$$v = \frac{\partial f}{\partial\rho} - \frac{\partial^2 f}{\partial\rho\partial g} g - \frac{\partial^2 f}{\partial^2 g}\frac{w}{g^2} - \frac{\partial f}{\partial g}\left(\frac{\nabla^2\rho}{g} - \frac{w}{g^3}\right). \tag{2.27}$$

Here ω is the second-order quantity defined as

$$w = \mathbf{g}^T \mathbf{H} \mathbf{g}, \tag{2.28}$$

where $\mathbf{g}$ and $\mathbf{H}$ given, respectively, by

$$\mathbf{g} = \begin{pmatrix} \dfrac{\partial \rho}{\partial x} \\ \dfrac{\partial \rho}{\partial y} \\ \dfrac{\partial \rho}{\partial z} \end{pmatrix} \tag{2.29}$$

and

$$\mathbf{H} = \begin{pmatrix} \dfrac{\partial^2 \rho}{\partial x^2} & \dfrac{\partial^2 \rho}{\partial x \partial y} & \dfrac{\partial^2 \rho}{\partial x \partial z} \\ \dfrac{\partial^2 \rho}{\partial y \partial x} & \dfrac{\partial^2 \rho}{\partial y^2} & \dfrac{\partial^2 \rho}{\partial y \partial z} \\ \dfrac{\partial^2 \rho}{\partial z \partial x} & \dfrac{\partial^2 \rho}{\partial z \partial y} & \dfrac{\partial^2 \rho}{\partial z^2} \end{pmatrix}. \tag{2.30}$$

Another common way of writing gradient-dependent density-functional approximations is

$$F[\rho] = \int f(\rho, s)\, d\mathbf{r}, \tag{2.31}$$

where s is the reduced (dimensionless) density gradient defined as

$$s \equiv \frac{|\nabla \rho|}{\rho^{4/3}}. \tag{2.32}$$

For such functionals, Eq. (1.30) becomes

$$v = \frac{\partial f}{\partial \rho} + \frac{\partial f}{\partial s}\left(\frac{h}{s^3} - \frac{q}{s}\right)\frac{1}{\rho} - \frac{\partial^2 f}{\partial \rho \partial s} s + \frac{\partial^2 f}{\partial s^2}\left(\frac{4}{3}s^2 - \frac{h}{s^2}\right)\frac{1}{\rho}, \tag{2.33}$$

where the second-order dimensionless quantities q and h are defined in the following way:

$$q = \frac{\nabla^2 \rho}{\rho^{5/3}} \tag{2.34}$$

and

$$h = \frac{w}{\rho^{13/3}}. \tag{2.35}$$

Initially, we wanted to test our implementation of the aufbau paths on potentials which are assured to be integrable. We derived two such potentials from the exchange functional proposed by Gill [34] and from the exchange part of the exchange-correlation functional of Perdew, Burke and Ernzerhof [35], $E_{\mathrm{x}}^{\mathrm{PBE}}[\rho]$. The Gill functional $E_{\mathrm{x}}^{\mathrm{G96}}[\rho]$ has a very simple form. It consists of the local density functional $E_{\mathrm{x}}^{\mathrm{LDA}}[\rho]$ and the gradient-correction term:

$$E_{\mathrm{x}}^{\mathrm{G96}}[\rho] = E_{\mathrm{x}}^{\mathrm{LDA}}[\rho] - b \int \rho^{-2/3}\, g^{3/2}\, d\mathbf{r}, \tag{2.36}$$

where $b = (2^{1/6})/137$ is an empirical parameter fitted in a way that $E_{\mathrm{x}}^{\mathrm{G96}}[\rho]$ reproduces the exact exchange energy of the Ar atom. We derived the potential corresponding to the Gill functional by using Eq. (2.27):

$$v_{\mathrm{x}}^{\mathrm{G96}} = v_{\mathrm{x}}^{\mathrm{LDA}} - b\,\rho^{-2/3} g^{-1/2} \left[\frac{1}{3}\rho^{-1} g^2 + \frac{3}{4} g^{-2} w - \frac{3}{2}\nabla^2 \rho \right]. \tag{2.37}$$

The Gill exchange potential lacks some analytic properties of the exact exchange potential. For example, $v_{\mathrm{x}}^{\mathrm{G96}}(\mathbf{r}) \to \infty$ as the distance from the atomic nucleus increases, while the exact potential vanishes in that limit. Nevertheless, the Gill functional performs reasonably well compared to many other gradient-dependent density-functional approximations.

The exchange functional of Perdew, Burke and Ernzerhof has the following form:

$$E_{\rm x}^{\rm PBE}[\rho] = E_{\rm x}^{\rm LDA}[\rho] - C_{\rm x}\int \rho^{4/3}\frac{\alpha k s^2}{k+\alpha s^2}\,d\mathbf{r}. \tag{2.38}$$

The constants α and k are non-empirical and are fixed by the requirements that Eq. (2.38) satisfies some exact constraints. For example, $E_{\rm x}^{\rm PBE}[\rho]$ correctly reduces to the uniform electron gas limit, $E_{\rm x}^{\rm LDA}[\rho]$, in the case of a homogeneous density. Numerical values of the constants are as follows: $k = 0.804$; $\alpha = m\mu$, where $m = (1/3\pi^2)^{2/3}/4$ and $\mu = 0.21951$. The expression for the corresponding potential can be written as

$$\begin{aligned} v_{\rm x}^{\rm PBE} &= v_{\rm x}^{\rm LDA} + \frac{2\alpha k}{3s^2(k+\alpha s^2)}v_{\rm x}^{\rm LDA} \\ &\times\left[2s^4+3h-3qs^2-\frac{4ks^4}{k+\alpha s^2}+\frac{k^3-2\alpha k^2 s^2-3\alpha k s^4}{(k+\alpha s^2)^3}\left(4s^4-3h\right)\right]. \end{aligned} \tag{2.39}$$

We obtained it using Eq. (2.33).

Next we list model potentials which were introduced directly, i.e., they are not derived from density functionals. As concluded in Ref. [27], all these potentials are actually non-integrable.

The van Leeuwen–Baerends exchange potential [7] has the form

$$v_{\rm x}^{\rm LB94} = v_{\rm x}^{\rm LDA} - \beta\left(\frac{\rho}{2}\right)^{1/3}\frac{x^2}{1+\beta\, s\,\mathrm{arcsinh}(x)}, \tag{2.40}$$

where $\beta = 0.05$ is an empirical parameter and $x = 2^{1/3}s$. This potential is designed to mimic the (exact) exchange-correlation potentials obtained from highly-accurate electron densities of Be and Ne atoms. The Slater potential [36]

$$v_{\rm x}^{\rm S}(\mathbf{r}) = -\frac{1}{2\rho(\mathbf{r})}\int d\mathbf{r}'\,\frac{|\rho(\mathbf{r},\mathbf{r}')|^2}{|\mathbf{r}-\mathbf{r}'|} \tag{2.41}$$

was introduced in 1951, before the advent of DFT, in the context of a simplification of the Hartree–Fock method. The symbol $\rho(\mathbf{r},\mathbf{r}')$ denotes the first-order spin-density matrix of the Kohn–Sham non-interacting system:

$$\rho(\mathbf{r},\mathbf{r}') = \sum_{i=1}^{\text{occ.}} \varphi_i(\mathbf{r})\varphi_i^*(\mathbf{r}'). \tag{2.42}$$

The potential of Becke and Johnson [19] is an improvement on the Slater potential:

$$v_{\text{x}}^{\text{BJ}} = v_{\text{x}}^{\text{S}} + \frac{k_{\text{BJ}}(\mathbf{r})}{2\pi}, \tag{2.43}$$

where

$$k_{\text{BJ}} = \left(\frac{5}{3}\frac{\tau}{\rho}\right)^{1/2}, \tag{2.44}$$

in which

$$\tau(\mathbf{r}) = \frac{1}{2}\sum_{i=1}^{\text{occ.}} |\nabla\varphi_i(\mathbf{r})|^2 \tag{2.45}$$

is the so-called kinetic-energy density. Along with quantities $g(\mathbf{r})$ and $s(\mathbf{r})$, the kinetic-energy density is a common ingredient of gradient-dependent density-functional approximations. The Becke–Johnson potential is designed to be exact for any hydrogen-like atom and it mimics well the shell structure of the exact exchange potential in many-electron atoms. The Umezawa potential [18]

$$v_{\text{x}}^{\text{U06}} = F(\mathbf{r})\, v_{\text{x}}^{\text{LDA}} + G(\mathbf{r})\, v_{\text{x}}^{\text{FA}} \tag{2.46}$$

is an interpolation between the LDA exchange potential, $v_{\text{x}}^{\text{LDA}}$, and the Fermi–Amaldi potential

$$v_{\text{x}}^{\text{FA}} = -\frac{1}{N}\int d\mathbf{r}'\, \frac{\rho(\mathbf{r}')}{|\mathbf{r}-\mathbf{r}'|}. \tag{2.47}$$

The latter being just a per-particle Coulomb potential of the electron density. The

switching functions

$$F(\mathbf{r}) = \frac{1}{\ln(1+\gamma^5 s^5)+1} \tag{2.48}$$

and

$$G(\mathbf{r}) = 1 - \exp\left(-\gamma^2 s^2\right) \tag{2.49}$$

are such that the Umezawa potential benefits from the reasonably good short-range behavior of the LDA potential, $v_{\mathrm{x}}^{\mathrm{LDA}}$, and from the correct asymptotic decay $(-1/r)$ of the Fermi–Amaldi potential, $v_{\mathrm{x}}^{\mathrm{FA}}$. The empirical parameter γ is chosen to be 0.125. The functions $F(\mathbf{r})$ and $G(\mathbf{r})$ are defined in terms of the spin-density, and the potentials $v_{\mathrm{x}}^{\mathrm{LDA}}$ and $v_{\mathrm{x}}^{\mathrm{FA}}$ are calculated from the total electron density.

2.4 Implementation of aufbau paths

Energy expressions for the aufbau paths [Eqs. (2.23) and (2.24)] involve one-dimensional integration over the parameter t and three-dimensional integration over the spatial coordinate $\mathbf{r}$. By considering the former as the outer integration, we can rewrite the energy expression for the orbital-aufbau path [Eq. (2.23)] in the following form:

$$E_{\mathrm{xc}}[\rho] = \int_0^N f(t)\, dt, \tag{2.50}$$

where $f(t)$ is the result of the inner integration

$$f(t) = \int v_{\mathrm{xc}}([\rho_t];\mathbf{r}) \frac{\partial \rho_t(\mathbf{r})}{\partial t}\, d\mathbf{r}. \tag{2.51}$$

The energy expression for the subshell-aufbau path [Eq. (2.24)] can be also rewritten in the same way, except that N will be replaced by N_s in Eq. (2.50).

In principle, any of various one-dimensional quadratures can be used to evaluate the outer integral. All of them require knowledge of the integrand $f(t)$ at some intermediate values of the parameter t. In the case of the aufbau path, the calculation

of $f(t)$ at each point t is itself an integration over $\mathbf{r}$.

The components needed to perform the inner integration are accessible from the development version of the GAUSSIAN quantum-chemistry program [37]. These components include a three-dimensional real-space grid and the corresponding weights as well as the values of Kohn–Sham orbitals and their first and second derivatives evaluated on that grid. We store all these components on disk together with some additional parameters, and then re-use them in our own newly written program, which we call `auprog`. `Auprog` calculates the value of the inner integral $f(t)$ for any intermediate value of t, which is needed to perform the outer integration.

We employ the Gauss–Legendre quadrature [38, 39] for the outer integration. We usually utilize grids containing $256 \times N$ points for the orbital-aufbau path and use $(256 \times N_s)$-point grids for the subshell-aufbau path. In the inner integration, we use the grid containing 300 radial and 974 spherical points per atom. This grid is requested in GAUSSIAN by the keyword `Int(Grid=299974)`. The grids for the outer integration give an accuracy of at least 4 decimal places. The inner (real-space) integration is more accurate, so the overall accuracy of exchange-correlation energies calculated in this Section is at least 4 decimal places.

In addition to the aufbau-path calculations, `auprog` is also capable of doing Q-path calculations. This is possible since the Q-path can be thought of as a subshell-aufbau path in which all the orbitals are considered as one subshell. We also implemented the Λ-path calculations in `auprog`. In addition, it is possible in `auprog` to use the parent functionals of those potentials that have them.

We put the detailed description of `auprog` in Appendix A.

2.5 Application of aufbau paths

To test our implementation of aufbau paths, we first applied it to two integrable potentials, $v_{\mathrm{x}}^{\mathrm{G96}}$ and $v_{\mathrm{x}}^{\mathrm{PBE}}$. The results are shown in Table 1. As one should expect,

Table 1: Total energies (in hartrees) calculated from various exchange potentials using the Λ-path, Q-path and the aufbau paths. All calculations are spin-unrestricted. The basis set used is cc-pVQZ.

	PBEx		G96		LB94				
	Functional	Any path	Functional	Any path	Λ-path	Q-path	Orbital aufbau	Subshell aufbau	Exact[a]
Atoms									
H	−0.4942	−0.4942	−0.4991	−0.4991	−0.4720	−0.6274	−0.6274	−0.6274	−0.5000
He	−2.8517	−2.8517	−2.8660	−2.8660	−2.8310	−3.3123	−3.3123	−3.3123	−2.9037
Li	−7.4100	−7.4100	−7.4308	−7.4308	−7.3744	−8.1939	−8.2115	−8.2115	−7.4781
Be	−14.5437	−14.5437	−14.5650	−14.5650	−14.5716	−15.7080	−15.7652	−15.7652	−14.6674
N	−54.3551	−54.3551	−54.3996	−54.3996	−54.7136	−56.9808	−57.2967	−57.2735	−54.5892
Ne	−128.5131	−128.5131	−128.5881	−128.5881	−129.6193	−133.0825	−133.8465	−133.7791	−128.9376
Na	−161.7988	−161.7988	−161.8827	−161.8827	−162.9406	−166.9881	−167.9010	−167.8164	−162.2546
P	−340.5860	−340.5860	−340.7198	−340.7198	−342.5895	−348.6035	−350.3189	−350.1666	−341.259
Ar	−526.6367	−526.6367	−526.8251	−526.8251	−529.4139	−537.0413	−539.4881	−539.2793	−527.540
Molecules									
H_2O (C_{2v})	−76.0589	−76.0589	−76.1134	−76.1134	−76.6606	−79.5131	−80.0772	−80.0772	−76.4087
CH_4 (T_d)	−40.1682	−40.1682	−40.2118	−40.21	−40.0108	−42.7203	−43.0166	−42.9926	−40.4921
NH_3 (C_{3v})	−56.2001	−56.20	−56.2473	−56.25	−56.4378	−59.1669	−59.6188	−59.6112	−56.5381

[a]For atoms the energies are taken from Refs. [40, 41]; for molecules, the exact energies are approximated by the CCSD(T,Full)/aug-cc-pV5Z values.

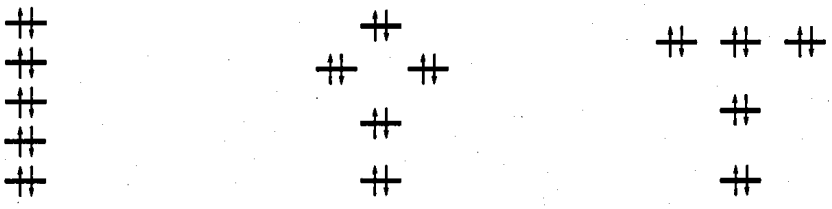

Fig. 1: Schematic structure of occupied energy levels in the water, ammonia and methane molecules.

the energies assigned via Λ-, Q- and aufbau paths are the same and equal to the energies obtained directly from the corresponding functionals $E_{\mathrm{x}}^{\mathrm{G96}}[\rho]$ and $E_{\mathrm{x}}^{\mathrm{PBE}}[\rho]$.

We also applied the aufbau paths to calculate the energies of the densities coming from the non-integrable model potentials of van Leeuwen–Baerends, $v_{\mathrm{x}}^{\mathrm{LB94}}$, and Umezawa, $v_{\mathrm{x}}^{\mathrm{U06}}$. The energy in both cases is path-dependent. The results for the van Leeuwen–Baerends potential are shown in Table 1, where we compare them to the results obtained from the Λ- and Q-paths. Generally, the energies calculated from the orbital- and subshell-aufbau paths are lower than those obtained from the Λ- and Q-paths. In addition, the aufbau-path energies tend to be lower than the exact ones.

As seen from Table 1, energies calculated from the orbital- and subshell-aufbau paths differ from each other for systems with degenerate orbitals (see the molecular orbital diagrams in Fig. 1). The difference is not as large as when aufbau paths are compared to other paths, but it is still noticeable. The orbital- and subshell-aufbau paths are in some sense close to each other and differ considerably from other paths, so the above result is reasonable.

In Fig. 2, we compare the dependence of the exchange energy on the number of electrons for integrable and non-integrable potentials. Both integrable potentials ($v_{\mathrm{x}}^{\mathrm{G96}}$ and $v_{\mathrm{x}}^{\mathrm{PBE}}$) give plots that are almost identical to each other, so we show only the results for the Perdew–Burke–Ernzerhof potential, $v_{\mathrm{x}}^{\mathrm{PBE}}$. Observe that the energy difference between integrable and non-integrable potentials increases with the number of electrons. Note also that the energies from the orbital- and subshell-aufbau paths

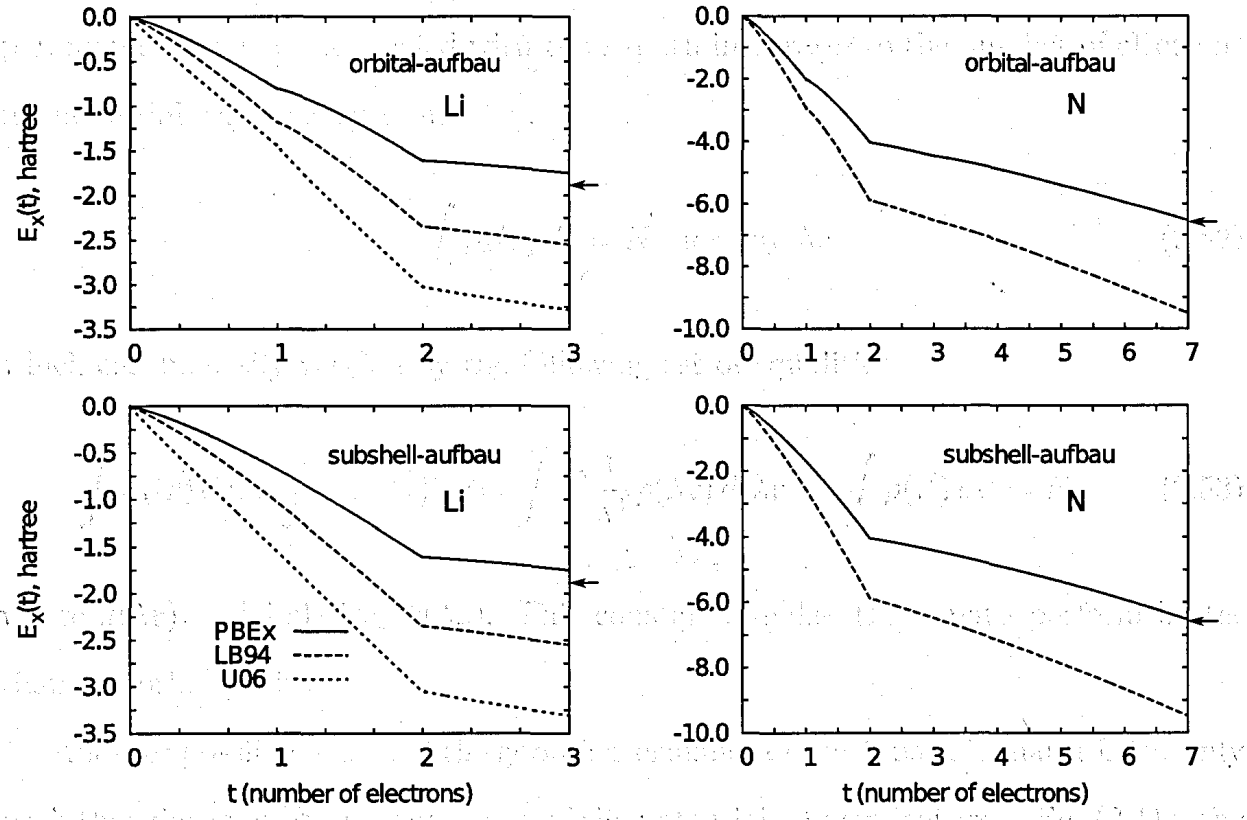

Fig. 2: Dependence of the exchange energy on the number of electrons in the lithium and nitrogen atoms for orbital- and subshell-aufbau paths. Arrows indicate exact exchange energies of the neutral atoms [42].

differ significantly from each other only in the range $0 \leq t \leq 2$.

As we discussed above, a combination of a density parametrization and a non-integrable model Kohn–Sham potential defines a new density-functional approximation. Our results indicate that, at least for the model potentials studied, the Λ-path performs better than all other paths, including the new aufbau paths. A possible explanation may be given if one observes the following special feature of the Λ-path. This path preserves the normalization of the density, that is, for any given value of the parameter λ, the density scaled with the Λ-path integrates to the number of electrons in the initial reference system:

$$\int \rho_\lambda(\mathbf{r})\, d\mathbf{r} = N \quad \text{for any } \lambda, \tag{2.52}$$

which can be easily verified by the following set of equalities

$$\int \rho_\lambda(\mathbf{r})\, d\mathbf{r} \equiv \int \lambda^3 \rho(\lambda\mathbf{r})\, d\mathbf{r} = \int \lambda^3 \frac{1}{\lambda^3} \rho(\lambda\mathbf{r})\, d(\lambda\mathbf{r}) = \int \rho(\mathbf{r}')\, d\mathbf{r}' = N, \tag{2.53}$$

where $d(\lambda\mathbf{r}) = d(\lambda x)\, d(\lambda y)\, d(\lambda z)$. This constancy makes the Λ-path perform better than the other paths.

Another possible reason of the good performance of the Λ-path is that it is the only path that does not change the shape of the potential. As evident from Eq. (2.11), the potential is just multiplied by a constant under the Λ-scaling. The coordinate scaling transformation $\mathbf{r} \longrightarrow \lambda\mathbf{r}$ only shrinks or stretches the potential but does not affect its shape.

In the future, it would be interesting to address the following challenge. For a given model potential, construct a path such that the density-functional approximation defined by the combination of potential and path, is as physical as possible. It appears that if a general way of doing this could be found, then it would be a fundamentally new approach for introducing approximations in density-functional theory.

3 Energies from model potentials: Janak path

In this Section we describe another possible way of assigning an energy value to a model potential. We obtain the corresponding energy expression and provide its alternative derivation from the line integral formula. We show the explicit form of the density parametrization that leads to this new energy expression.

3.1 DFT for non-integer electron numbers

We mentioned in the Introduction that the definition of the universal density functional [Eq. (1.8)],

$$F[\rho] = \min_{\Psi \to \rho} \langle \Psi | \hat{T} + \hat{V}_{\mathrm{ee}} | \Psi \rangle,$$

has to be extended for systems with degenerate ground states [3]. The extension is such that the minimization is done not only over all possible anti-symmetric N-electron wavefunctions Ψ but also over all possible *statistical mixtures (ensembles)* of such wavefunctions. In quantum mechanics, a statistical mixture is described by its own operator $\hat{\Gamma}$, $\hat{\Gamma} = \sum_i p_i |\Psi_i\rangle\langle\Psi_i|$. In this work we will not go into thorough discussion of this operator. However, we will use the symbol $\hat{\Gamma}$ to denote properties that correspond to an ensemble. This said, the universal density functional extended to ensembles is defined as

$$F[\rho] = \min_{\hat{\Gamma} \to \rho} \langle \Psi | \hat{T} + \hat{V}_{\mathrm{ee}} | \Psi \rangle_{\hat{\Gamma}}. \tag{3.1}$$

Here the expectation value $\langle \Psi | \hat{T} + \hat{V}_{\mathrm{ee}} | \Psi \rangle_{\hat{\Gamma}}$ of the statistical mixture of pure-state wavefunctions Ψ_i is given by

$$\langle \Psi | \hat{T} + \hat{V}_{\mathrm{ee}} | \Psi \rangle_{\hat{\Gamma}} \equiv \sum_i p_i \langle \Psi_i | \hat{T} + \hat{V}_{\mathrm{ee}} | \Psi_i \rangle, \tag{3.2}$$

where p_i is the contribution of the wavefunction Ψ_i to the ensemble $\hat{\Gamma}$, and

$$\sum_i p_i = 1 \quad \text{with} \quad 0 \leq p_i \leq 1. \tag{3.3}$$

The extension shown in Eq. (3.1) allows the density-functional theory to treat the so-called mixed states, i.e., the states that cannot be described by a single wavefunction. Examples of mixed states include systems with degeneracies and systems with fluctuating number of electrons. The latter may arise when wavefunctions corresponding to different numbers of electrons are included in the statistical mixture $\hat{\Gamma}$. The systems with non-integer electron numbers may be thought of as statistical averages of the systems which are free to exchange electrons with the surrounding (open systems).

The Kohn–Sham method can be extended to handle non-integer electron numbers. This is done by introducing fractional occupation numbers $0 < n_i \leq 1$ into the expression for the electron density,

$$\rho = \sum_{i=1}^{N} n_i |\varphi_i|^2, \tag{3.4}$$

and into the expression for the kinetic energy of non-interacting electrons

$$T_s = -\frac{1}{2} \sum_{i=1}^{N} n_i \langle \varphi_i | \nabla^2 | \varphi_i \rangle. \tag{3.5}$$

For systems extended in such a way, Janak showed [43] that the response of the total energy to a change in the occupation number of the i-th orbital is equal to the energy of that orbital:

$$\frac{\partial E}{\partial n_i} = \epsilon_i. \tag{3.6}$$

This result is known as the Janak theorem.

The Janak theorem plays an important role in the later derivations, so for the sake of completeness, we give its proof here. To begin with, consider the following

derivative

$$\frac{\partial E}{\partial n_i} = \frac{\partial}{\partial n_i} T_s + \frac{\partial}{\partial n_i} \left(J[\rho] + E_{\text{xc}}[\rho] + E_{\text{ne}}[\rho] \right), \tag{3.7}$$

where T_s is in its extended form [Eq. (3.5)], $J[\rho]$ and $E_{\text{xc}}[\rho]$ are the same as defined by Eqs. (1.16) and (1.15), and $E_{\text{ne}}[\rho]$ is the electron-nuclear attraction term

$$E_{\text{ne}}[\rho] \equiv \int v(\mathbf{r}) \rho(\mathbf{r}) \, d\mathbf{r} \tag{3.8}$$

with the external potential $v(\mathbf{r})$ given by Eq. (1.5). Let us start by working out the first term of Eq. (3.7):

$$\frac{\partial}{\partial n_i} T_s = -\frac{1}{2} \frac{\partial}{\partial n_i} \sum_{j=1}^{N} n_j \langle \varphi_j | \nabla^2 | \varphi_j \rangle = -\frac{1}{2} \langle \varphi_i | \nabla^2 | \varphi_i \rangle - \frac{1}{2} \sum_{j=1}^{N} n_j \frac{\partial}{\partial n_i} \langle \varphi_j | \nabla^2 | \varphi_j \rangle. \tag{3.9}$$

The above result can be written in a more compact way if we introduce the following notation for the orbital kinetic-energy integrals:

$$t_j = -\frac{1}{2} \langle \varphi_j | \nabla^2 | \varphi_j \rangle. \tag{3.10}$$

With this notation Eq. (3.9) becomes

$$\frac{\partial}{\partial n_i} T_s = t_i + \sum_{j=1}^{N} n_j \frac{\partial}{\partial n_i} t_j. \tag{3.11}$$

Now let us work out the second part of Eq. (3.7). Functionals $J[\rho]$, $E_{\text{xc}}[\rho]$, and $E_{\text{ne}}[\rho]$ are simultaneously functions of all occupation numbers n_i. So the chain rule needs to be applied in order to calculate necessary derivatives:

$$\begin{aligned} \frac{\partial}{\partial n_i} \left(J[\rho] + E_{\text{xc}}[\rho] + E_{\text{ne}}[\rho] \right) &= \int \frac{\delta}{\delta \rho} \left(J[\rho] + E_{\text{xc}}[\rho] + E_{\text{ne}}[\rho] \right) \frac{\partial \rho}{\partial n_i} \, d\mathbf{r} \\ &= \int v_s(\mathbf{r}) \left(|\varphi_i|^2 + \sum_{j=1}^{N} n_j \frac{\partial}{\partial n_i} |\varphi_j|^2 \right) d\mathbf{r}, \end{aligned} \tag{3.12}$$

where $v_s = (v_J + v + v_{\mathrm{xc}})$ is the Kohn–Sham potential as introduced in Eq. (1.18). Combining the results of Eqs. (3.11) and (3.12), and rearranging the terms, we cast Eq. (3.7) in the following form:

$$\frac{\partial E}{\partial n_i} = t_i + \int v_s |\varphi_i|^2 \, d\mathbf{r} + \sum_{j=1}^{N} n_j \left(\frac{\partial}{\partial n_i} t_j + \int v_s \frac{\partial}{\partial n_i} |\varphi_j|^2 \, d\mathbf{r} \right). \tag{3.13}$$

Let us now consider the Kohn–Sham equations [Eq. (1.21)]

$$\left(-\frac{1}{2}\nabla^2 + v_J + v + v_{\mathrm{xc}} \right) \varphi_i = \epsilon_i \varphi_i.$$

If we multiply them by φ_i^* and integrate over the spatial coordinates—a common trick used in quantum mechanics—we will find the relation

$$t_i + \int v_s \, |\varphi_i|^2 \, d\mathbf{r} = \epsilon_i. \tag{3.14}$$

The above equation brings Eq. (3.13) into a simpler form

$$\frac{\partial E}{\partial n_i} = \epsilon_i + \sum_{j=1}^{N} n_j \left(\frac{\partial}{\partial n_i} t_j + \int v_s \frac{\partial}{\partial n_i} |\varphi_j|^2 \, d\mathbf{r} \right). \tag{3.15}$$

By spelling out the symbol t_j and by taking the partial derivatives with respect to n_i, we see that the sum in parenthesis is equal to zero:

$$\begin{aligned} \frac{\partial}{\partial n_i} t_j + \int v_s \frac{\partial}{\partial n_i} |\varphi_j|^2 \, d\mathbf{r} &= \int \left(\frac{\partial}{\partial n_i} \varphi_j^* \right) \left(-\tfrac{1}{2}\nabla^2 + v_s \right) \varphi_j \, d\mathbf{r} + \text{complex conjugate} \\ &= \int \left(\frac{\partial}{\partial n_i} \varphi_j^* \right) \epsilon_j \varphi_j \, d\mathbf{r} + \text{complex conjugate} \\ &= \epsilon_j \frac{\partial}{\partial n_i} \int |\varphi_j|^2 \, d\mathbf{r} = \epsilon_j \frac{\partial}{\partial n_i} 1 = 0, \end{aligned} \tag{3.16}$$

where we exploited the fact that Kohn–Sham orbitals are normalized. The result of Eq. (3.16) makes the summation over j in Eq. (3.15) vanish. The last step brings

Eq. (3.15) to the expression obtained by Janak [Eq. (3.6)], and completes the proof.

Janak's work dates back to the time when researchers in density-functional theory were trying to minimize the total-energy density functional $E[\rho]$ not only with respect to the density but also with respect to the occupation numbers. Now we know that there is not as much freedom in values of the occupation numbers as was assumed in the earlier days. For instance, Valiev and Fernando showed [44] that only the highest-occupied orbital or orbitals, if they are degenerate, are allowed to have fractional occupations. All the lower-energy orbitals must be fully occupied. The reason being is that $T_s[\rho]$ and $E_{\rm xc}[\rho]$ are differentiable only when the above constraint is satisfied.

Janak suggested using Eq. (3.6) as a way of calculating the energy of the first excited state of a system [43]. Integration of Eq. (3.6) over the occupation number n_{N+1} gives

$$E_{N+1} = E_N + \int_0^1 \epsilon(n_{N+1})\, dn_{N+1}. \tag{3.17}$$

If E_N is known, then E_{N+1} can be obtained by integration of the energy of the $(N+1)$-th orbital with respect to its occupation number n_{N+1}. In the late 1970s, it was a computationally involved procedure to obtain a lot of intermediate points to calculate the integral of Eq. (3.17). So Janak, following Slater [45], considered an approximation of the integral by a single point $n_{N+1} = 1/2$. This approximation turns out to be quite reasonable. We will discuss it in greater detail in Section 4. For now, let us show how the Janak theorem can be used to assign an energy to a model potential.

3.2 Energy expression based on the Janak theorem

Suppose we are given a model exchange-correlation potential for an N-electron system and we want to find the associated energy. First, let us rewrite Eq. (3.17) in a slightly different form that shows explicitly how one can use the Janak theorem to calculate

energy differences:

$$E_N - E_{N-1} = \int_0^1 \epsilon(n_N)\, dn_N. \tag{3.18}$$

Now, if we apply Eq. (3.18) to the N-th orbital while keeping all lower-lying orbitals fully occupied and all higher-lying orbitals empty, we will get the energy difference $(E_N - E_{N-1})$. Doing the same procedure for the 1-st, 2-nd, 3-rd, ..., N-th orbitals, we will obtain, respectively, the energy differences $(E_1 - E_0)$, $(E_2 - E_1)$, $(E_3 - E_2)$, ..., $(E_N - E_{N-1})$. Adding them up results in a telescopic cancellation of all the intermediate absolute-energy values E_i except for E_0 and E_N:

$$(E_1 - E_0) + (E_2 - E_1) + \cdots + (E_N - E_{N-1}) = E_N - E_0. \tag{3.19}$$

The term E_0 corresponds to the system with no electrons. Such system has zero energy, $E_0 = 0$, so only the term E_N survives. In other words, by following the procedure outlined above, it is possible to assign an energy E_N to a model exchange-correlation potential without actually knowing the explicit expression of the functional. The method requires only knowledge of the energy of the highest-occupied molecular orbital (HOMO) as a function of its occupation number for all intermediate systems that arise when the number of electrons changes form 0 to N. This result can be thought of as the generalization of the Janak theorem. To the best of our knowledge, there is no discussion in the literature of this way of extracting the energy from model Kohn–Sham potentials.

The formal expression for the procedure outlined above can be written as

$$E_N = \sum_{i=1}^{N} \int_0^1 d\omega\, \epsilon_{\mathrm{HOMO}}(i, \omega), \tag{3.20}$$

where $\epsilon_{\mathrm{HOMO}}(i, \omega)$ denotes the energy of the highest-occupied molecular orbital of the system in which the lower $(i-1)$ orbitals are fully occupied and the i-th orbital, the

HOMO, has an occupation number equal to ω.

Let us also provide an alternative argument leading to the same result as Eq. (3.20). For a system in which only the HOMO is allowed to have fractional occupations and in which all the lower-energy orbitals are fully occupied, a change in the occupation number of that orbital, $\partial n_{\mathrm{HOMO}}$, is equivalent to the change of the total number of electrons, ∂N. In this case, the Janak theorem reads

$$\epsilon_{\mathrm{HOMO}}(t) = \frac{\partial E}{\partial N}. \tag{3.21}$$

Here by $\epsilon_{\mathrm{HOMO}}(t)$ we mean a collective representation of the energy of the highest-occupied molecular orbitals. That is, $\epsilon_{\mathrm{HOMO}}(t)$ always represents the HOMO energy regardless of the ordinal (serial) number of that orbital. With this definition, one just needs to integrate equation (3.21) in order to get the expression for the total energy:

$$E_N = \int_0^N \epsilon_{\mathrm{HOMO}}(t)\, dt. \tag{3.22}$$

Now, if we take into account the fact that there are N orbitals in an N-electron system, and that each of them becomes the HOMO at some stage in the electron addition process, it is evident that Eq. (3.22) is just another way of writing Eq. (3.20).

The way of extracting the energies from model potentials described above and Eq. (3.22) in particular, resembles the line integration technique which we have described in Section 2. This analogy motivated us to investigate the density parametrization that lies behind the energy expression of Eq. (3.22), or, rather, identify the parametrization that is implicitly present in Janak's original paper [43].

The manner in which the orbital energy $\epsilon_{\mathrm{HOMO}}(t)$ is calculated suggests that there is always a unique combination of i and ω from Eq. (3.20) that corresponds to some particular value of t. Specifically, the value is $t = i + \omega$. Since ω is always within the range from 0 to 1, and since i is an integer number, we can think of i as the integer

part of the parameter t, $i = \lfloor t \rfloor$, and ω as the fractional part, $\omega = \{t\}$. Then it immediately becomes clear what density parametrization corresponds to Eqs. (3.22) and (3.20). The parametrization, which we call the *Janak path*, can be written as

$$\rho_t(\mathbf{r}) = \sum_{i=1}^{\lfloor t \rfloor} |\varphi_i(\mathbf{r})|^2 + \{t\}|\varphi_{\lfloor t+1 \rfloor}(\mathbf{r})|^2. \tag{3.23}$$

The Janak path is formally similar to the orbital-aufbau path discussed in Section 2, except that Kohn–Sham orbitals are no longer fixed here. They depend on t, i.e., they are re-calculated self-consistently for each value of t. Because of that, the Janak path is more complex than the orbital-aufbau path. For this reason, it is impossible to prove the continuity of ρ_t as we did for the aufbau paths. It is also impossible to evaluate explicitly the derivative $\dfrac{\partial \rho_t}{\partial t}$. But this is not needed since we already know the energy expression that corresponds to the Janak path.

Let us now show that Eq. (3.22) can be also viewed as a special case of the van Leeuwen–Baerends line integration formula [Eq. (2.5)]. We begin by rewriting Eq. (2.5) as

$$E_N = \int_0^N dt \int d\mathbf{r} \frac{\delta E[\rho_t]}{\delta \rho_t(\mathbf{r})} \frac{\partial \rho_t(\mathbf{r})}{\partial t}. \tag{3.24}$$

Here we have already identified the integration domain, $0 \leq t \leq N$, because we know that it is the same as in the Janak path. The generalization of the line integral formula for calculations of the total energy is a valid procedure since the total energy is a functional of the electron density.

The first factor of the integrand in Eq. (3.24) is the chemical potential μ, defined in density-functional theory by [46]:

$$\mu(t) = \frac{\delta E[\rho_t]}{\delta \rho_t(\mathbf{r})}. \tag{3.25}$$

An alternative expression for chemical potential is:

$$\mu = \frac{\partial E}{\partial N}, \tag{3.26}$$

which becomes the energy of the highest-occupied molecular $[\epsilon_{\text{HOMO}}(t)]$ when only the HOMO's occupation number (n_{HOMO}) is allowed to be fractional. With this in mind, we can write the following sequence of equalities:

$$\frac{\delta E[\rho_t]}{\delta \rho_t(\mathbf{r})} = \mu(t) = \frac{\partial E}{\partial N} = \frac{\partial E}{\partial n_{\text{HOMO}}} = \epsilon_{\text{HOMO}}(t). \tag{3.27}$$

Thorough discussion of the chemical potential μ is beyond the scope of this work, so we just quoted the above results from the literature. See, for example, Ref. [5].

To proceed with our investigation of Eq. (3.22), observe the following two important consequences of Eq. (3.27). The first is that

$$\frac{\delta E[\rho_t]}{\delta \rho_t(\mathbf{r})} = \epsilon_{\text{HOMO}}(t) \tag{3.28}$$

and the second is that $\epsilon_{\text{HOMO}}(t)$ is a function of t only, even though it is a functional derivative. These two facts allow us to factor $\epsilon_{\text{HOMO}}(t)$ out of the spatial integral in Eq. (3.24):

$$E_N = \int_0^N dt \left[\epsilon_{\text{HOMO}}(t) \int d\mathbf{r}\, \frac{\partial \rho_t(\mathbf{r})}{\partial t}\right]. \tag{3.29}$$

Note that Eq. (3.29) differs from the energy expression of Eq. (3.22) only by the presence of the spatial integral of $\frac{\partial \rho_t}{\partial t}$ in the latter. As discussed above, this derivative alone cannot be evaluated due to implicit dependence of Kohn–Sham orbitals on the

parameter t. However, the spatial integral of this derivative can be easily evaluated:

$$\begin{aligned}\int d\mathbf{r}\,\frac{\partial\rho_t(\mathbf{r})}{\partial t} &= \int d\mathbf{r}\,\frac{\partial}{\partial t}\left(\sum_{i=1}^{\lfloor t\rfloor}|\varphi_i(\mathbf{r})|^2+\{t\}\,|\varphi_{\lfloor t\rfloor+1}(\mathbf{r})|^2\right) \\ &= \frac{\partial}{\partial t}\left(\sum_{i=1}^{\lfloor t\rfloor}\int|\varphi_i(\mathbf{r})|^2\,d\mathbf{r}+\{t\}\int|\varphi_{\lfloor t\rfloor+1}(\mathbf{r})|^2\,d\mathbf{r}\right) \\ &= \frac{\partial}{\partial t}\left(\sum_{i=1}^{\lfloor t\rfloor}(1)+\{t\}\right) = \frac{\partial}{\partial t}\left(\lfloor t\rfloor+\{t\}\right) = \frac{\partial}{\partial t}t = 1,\end{aligned} \tag{3.30}$$

where we exploited the fact that each Kohn–Sham orbital is normalized,

$$\int d\mathbf{r}\,|\varphi_i(\mathbf{r})|^2 = 1. \tag{3.31}$$

The result of Eq. (3.30) shows how Eq. (3.29) and, consequently, Eq. (3.24) reduces to Eq. (3.22). In other words, we have just demonstrated that the energy expression derived from the Janak theorem is indeed the result of application of the van Leeuwen–Baerends line integration taken along the Janak path. We will call the energy assigned to a potential via Eq. (3.20) or, equivalently, via Eq. (3.22) the Janak-path energy.

3.3 Performance of the Janak path

To test Eq. (3.20) numerically, we ran a number of calculations with the Gill exchange potential ($v_{\mathrm{x}}^{\mathrm{G96}}$) and the exchange potential of Perdew, Burke, and Ernzerhof ($v_{\mathrm{x}}^{\mathrm{PBE}}$). As discussed in Section 2, these two potentials are integrable as they are both derived from the corresponding functionals $E_{\mathrm{x}}^{\mathrm{G96}}[\rho]$ and $E_{\mathrm{x}}^{\mathrm{PBE}}[\rho]$. For integrable potentials one can expect that the energies obtained from Eq. (3.20) and from the corresponding functional would coincide, apart from numerical integration errors. That is precisely what we observed in our calculations (see Table 2). This means that Eq. (3.20) is indeed another possible way of assigning an energy to a potential.

Table 2: Total energies (in hartrees) calculated via the Janak path from integrable model potentials. The basis set used is cc-pVQZ.

	G96		PBEx	
	Janak-path	Functional	Janak-path	Functional
H	−0.499 051	−0.499 052	−0.494 165	−0.494 165
He	−2.865 954	−2.865 956	−2.851 694	−2.851 694
Ne	−128.588 115	−128.588 126	−128.513 092	−128.513 090

We applied Eq. (3.20) to the non-integrable potentials of Umezawa ($v_{\mathrm{x}}^{\mathrm{U06}}$), van Leeuwen and Baerends ($v_{\mathrm{x}}^{\mathrm{LB94}}$), Slater ($v_{\mathrm{x}}^{\mathrm{S}}$), and Becke and Johnson ($v_{\mathrm{x}}^{\mathrm{BJ}}$)—see the results in Table 3. We compare the Janak-path energies calculated from these potentials to the Λ-path energies computed via the Levy–Perdew virial formula [Eq. (2.12)]. In some cases, the Janak-path energies are better than the ones obtained from the virial formula, as in the case of the hydrogen atom and the Umezawa potential. For the Slater potential, the Janak-path and Λ-path energies almost coincide. Generally, however, the Levy–Perdew (Λ-path) energies are still closer to the exact values.

Compared to the aufbau path, calculation of Janak-path energies is computationally more involved. To calculate an energy by Eq. (3.20), we generally use a $(256 \times N)$-point Gauss–Legendre quadrature. Specifically, for each integer i, we calculate the HOMO energy, $\epsilon_{\mathrm{HOMO}}(i, \omega)$, at 256 intermediate points of ω and then integrate it. Since i varies from 0 to N, the total number of quadrature points adds up to $256 \times N$. Each such point requires a separate self-consistent solution of the Kohn–Sham equations. In many cases, we experienced problems with convergence, which is why the amount of data for Janak-path calculations (Table 2 and Table 3) is less than that for the aufbau paths (Table 1).

On Fig. 3 we show how the energy of the highest-occupied molecular orbital depends on the number of electrons in the helium atom. The area above each line is the Janak-path energy. The exact potential would be a set of horizontal segments with jumps at integer points (see the solid bold line). Among potentials tested, only the Slater ($v_{\mathrm{x}}^{\mathrm{S}}$) and Becke–Johnson ($v_{\mathrm{x}}^{\mathrm{BJ}}$) potentials, and only in the region $0 \leq t \leq 1$

Table 3: Total energies (in hartrees) calculated from various exchange potentials via the Janak and Λ- paths.

		Umezawa		LB94		Slater		Becke–Johnson	
	Exact[a]	Janak path	Λ-path	Janak path	Λ-path	Janak path	Λ-path	Janak path	Λ-path
H	−0.5000	−0.5072	−0.3913	−0.6405	−0.4720	−0.4999	−0.4999	−0.2945	−0.5001
He	−2.9037	−3.2236	−2.7256	−3.3767	−2.8310	−2.8615	−2.8614	−2.1239	−2.7795
Li	−7.4781	−8.0868	−7.1758	−8.2953	−7.3744	n/c		n/c	
Be	−14.6674	−15.6608	−14.2451	−15.8837	−14.5716	n/c		n/c	

[a]Exact nonrelativistic energies are taken from Refs. [40, 41].

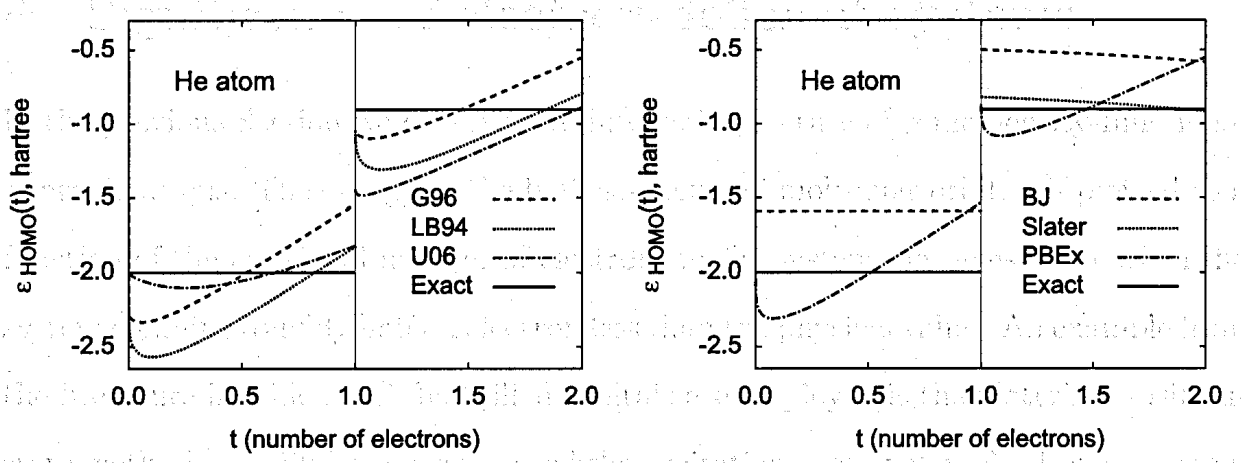

Fig. 3: Energy of the HOMO as a function of the number of electrons in the He atom. The HOMO energy is calculated at 256×2 intermediate values of t. The basis set used is cc-pVQZ.

mimic this behavior. Everywhere else the tested potentials fail to mimic even qualitatively the behavior of the exact potential. Note also an interesting feature of the Gill and Perdew–Burke–Ernzerhof potentials. The orbital energy for these potentials becomes almost exact when it is calculated at half-integer values of t.

To conclude the computational part of this Section, the Janak-path calculations are numerically more expensive as they require a separate self-consistent solution of the Kohn–Sham equations for each value of the parameter t. For this reason the Janak path is not very practical for routine calculations. The Janak path, however, enabled us to observe an interesting feature of some density-functional approximations, namely, the tendency of the HOMO energy to cross the exact value near the point $t = N - 1/2$, i.e., at approximately half an electron less than the actual system of interest. We will return to this issue in the next Section.

4 Significance of electron-deficient systems

In the previous Section we observed an interesting feature of some density-functional approximations. The energy of the highest-occupied molecular orbital, if plotted as a function of the fractional number of electrons in the system, becomes exact when the system contains roughly half an electron less than the physical value. An example from the literature in which such half-filled orbitals are employed is the Slater's transition-state method [45]. Slater approximated the excitation energy of an N-electron system by a single calculation on a system containing $(N + 1/2)$ electrons. Also, Dabo and co-workers [47] recently proposed an approximate density functional that involves half-electron deficient densities. All these examples suggest that an auxiliary system that differs from the system of interest by half an electron possesses important information about the corresponding system with the integer electron number. The purpose of this Section is to investigate what is special about such fractionally charged systems and to see how one can exploit these systems. In particular, we will address the problem of predicting the ionization energies in density-functional theory.

4.1 Ionization energy in density-functional theory

In 1982, Perdew, Parr, Levy and Balduz [48] showed that in the *exact* density functional theory, the total energy is a continuous piecewise-linear function of the number of electrons. This linearity follows from the analysis of statistical mixtures (ensembles) of pure-state wavefunctions corresponding to different electron numbers [5, 46, 48]. Suppose for a moment that the mixture contains only the $(J-1)$- and J-electron states (where J is an integer). Then the electron density of this mixture, $\rho_{J-\omega}$, is given by

$$\rho_{J-\omega} = (1-\omega)\,\rho_J + \omega\,\rho_{J-1}, \tag{4.1}$$

where $(1-\omega)$ and ω are weights of the J- and $(J-1)$-electron states, respectively, and ρ_J and ρ_{J-1} are the electron densities of these states. The parameter ω is in the range between 0 and 1. If $\omega = 0$, then the ensemble reduces to the pure J-electron state, and if $\omega = 1$, to the $(J-1)$-electron state. Careful analysis shows that the energy $E_{J-\omega}$ of the above ensemble is [48]

$$E_{J-\omega} = (1-\omega)\, E_J + \omega E_{J-1}, \tag{4.2}$$

where E_J and E_{J-1} are the energies of the corresponding pure states. Equation (4.2) can be rearranged to reveal the linearity of the energy of the ensemble:

$$E_{J-\omega} = -\left(E_J - E_{J-1}\right)\omega + E_J. \tag{4.3}$$

Equation (4.2) is a general result in density-functional theory [48]. It holds for any types of mixtures, even those that include other states that are different from the J- and $(J-1)$-electron states. This result remains general in DFT as long as the condition

$$2E_J < E_{J-1} + E_{J+1} \tag{4.4}$$

is satisfied. This inequality is an assumption that has never been shown to be violated (theoretically and experimentally), at least for electrons. We will see soon that the linearity of the total energy leads to an important expression for the ionization energy in the exact density functional theory.

The first ionization energy is defined as the lowest energy required to remove an electron from the system. In other words, the ionization energy I_J of a J-electron system is the energy difference between the ground-state energy of that system, E_J, and the ground-state energy of the corresponding system with one electron removed, E_{J-1}:

$$I_J \equiv E_{J-1} - E_J. \tag{4.5}$$

Ionization energy as defined in Eq. (4.5) is a positive number, provided that $E_J < E_{J-1}$, which is always the case for a neutral J-electron system. It is evident from Eq. (4.3) that the slope of the total energy $E_{J-\omega}$ is the negative of the ionization energy:

$$\frac{\partial E_{J-\omega}}{\partial \omega} = -(E_{J-1} - E_J) = -I_J. \tag{4.6}$$

The slope can be calculated at any ω in the range from 0 to 1.

A common practice in the Kohn–Sham density-functional theory is to *estimate* the ionization energy by the energy of the highest-occupied molecular orbital, $\epsilon_{\text{HOMO}}(J)$:

$$I_J = -\epsilon_{\text{HOMO}}(J). \tag{4.7}$$

We know from the Janak theorem that if all the lower-energy orbitals are fully occupied and only the HOMO has a fractional occupation, the HOMO energy is given by

$$\epsilon_{\text{HOMO}} = \frac{\partial E}{\partial N}. \tag{4.8}$$

In view of Eq. (4.6), the above equation can be rewritten as

$$I_J = -\frac{\partial E_{J-\omega}}{\partial \omega}. \tag{4.9}$$

If one estimates the ionization energy by Eq. (4.7), one in fact estimates it as the following limit:

$$I_J = \lim_{\omega \to 0+} \frac{\partial E_{J-\omega}}{\partial \omega} \tag{4.10}$$

or, equivalently,

$$I_J = \lim_{N \to J-} \frac{\partial E}{\partial N}. \tag{4.11}$$

If the limits of Eqs. (4.10) or (4.11) were calculated from the exact total-energy functional, then the ionization energy obtained from these equations would be exact.

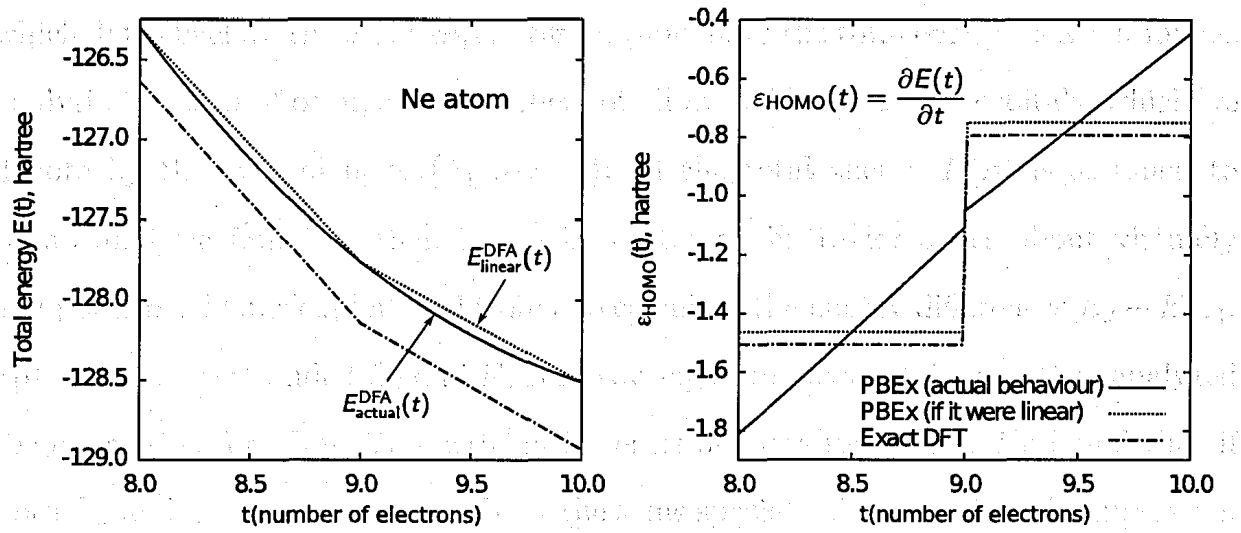

Fig. 4: Dependence of the total energy, $E(t)$, and the energy of the highest-occupied molecular orbital, $\epsilon_{\rm HOMO}(t)$, on the number of electrons for the Ne atom in the exact density functional theory and as obtained from the approximate exchange functional of Perdew, Burke and Ernzerhof. Many other density-functional approximations (DFA) behave similarly. The basis set used is cc-pVQZ. The number of intermediate points between any two adjacent integer values of t is 256.

Currently available density-functional approximations, however, are not able to predict exact ionization energies. They tend to underestimate them by as much as dozens of percent. One of the reasons is that density-functional approximations are not linear functions of the number of electrons. Most often they exhibit convex plots for the total energy $E(t)$ as a function of the electron number t. For example, see Fig. 4 where we show the results of actual calculations (solid line). Because of the non-linearity of $E(t)$, the most accurate estimate of the ionization potential I_J is not necessarily calculated from the J-electron system. As Fig. 4 suggests, the best estimate should be expected from the system with an electron number that is close to $(J-1/2)$. The plot of the orbital energy versus the number of electrons on the right-hand side panel of Fig. 4 also suggests that the orbital energy calculated from a density-functional approximation is close to a linear function. This implies that the total energy $E(t)$ is a quadratic function of the number of electrons.

Another possible way of calculating the energy difference between the J- and $(J-1)$-electron states of a system is the Slater transition state method [45, 49, 50],

which dates back to the early 1970s. Slater thought of the total energy as a continuous analytic function of occupation numbers of all available molecular orbitals, which we denote by the symbol $\mathbf{n} \equiv \{n_1, n_2, \ldots\}$. If the total energy $E(\mathbf{n})$ is assumed to be an analytic function, then it can be expanded in Taylor series about virtually any point $\mathbf{n}_0$. Slater exploited this fact to calculate the energy differences $E_J - E_{J-1}$. Specifically, he expanded E_J and E_{J-1} in two separate Taylor series and then analyzed the expression for $E_J - E_{J-1}$ written in terms of these two series. He found that if both E_J and E_{J-1} are expanded about the same special point $\mathbf{n}_{\mathrm{TS}}$, then the expression for the energy difference is greatly simplified:

$$E_J - E_{J-1} = \left.\frac{\partial E(\mathbf{n})}{\partial n_J}\right|_{\mathbf{n}_{\mathrm{TS}}} + \{\text{3rd- and higher odd-order terms}\}. \tag{4.12}$$

The first term in Eq. (4.12) dominates by at least one order of magnitude, as Slater and Wood showed [49] in calculations for the chromium atom. The special point $\mathbf{n}_{\mathrm{TS}}$ is such that all $(J-1)$ lower-energy orbitals are fully occupied and the J-th orbital has only half an electron in it. The system that corresponds to the point $\mathbf{n}_{\mathrm{TS}}$ is called a transition state since it is in the middle of the "transition" of the system from the J- to $(J-1)$-electron states, i.e., it has a half-filled HOMO. In other words, the transition state is an auxiliary system containing half an electron less than the original J-electron system. If the transition from the J- to $(J+1)$-electron state were considered, then the transition state would correspond to the $(J+1/2)$-electron system.

The partial derivative in Eq. (4.12) is precisely the orbital energy of the $(J-1/2)$-electron system. So, according to the transition-state method, the ionization energy of a J-electron system is equal (up to a sign) to the energy of the highest-occupied molecular orbital calculated from the $(J-1/2)$-electron system. Slater's result is similar to what we observed by analyzing how the HOMO energy depends on the electron number. This fact, in general, brings new insights to the Slater

transition state method. In what follows, we will investigate numerically the behavior of the total energy as a function of the electron number for some density-functional approximations. We will demonstrate how the Slater's result naturally arises from the analysis of the deviation of approximate functionals from the linearity.

4.2 Single-point approximations to ionization energies

As seen from Fig. 4, the total energy $E^{\mathrm{DFA}}_{\mathrm{actual}}(t)$ calculated from some density-functional approximation ($E^{\mathrm{PBE}}_{\mathrm{x}}[\rho]$ in this case) deviates from linearity. More precisely, the energy is convex between any two adjacent integer values of t. So the problem we are going to address first is to determine the magnitude of these deviations and their shape. In particular, we would like to know how close the deviations are to a quadratic function. To that purpose, we introduce a function $E^{\mathrm{DFA}}_{\mathrm{linear}}(t)$, which we *define* as a piecewise-linear function connecting the total energies calculated at integer values of t (see Fig. 4). We then study the deviation $D(t)$ defined as

$$D(t) \equiv E^{\mathrm{DFA}}_{\mathrm{actual}}(t) - E^{\mathrm{DFA}}_{\mathrm{linear}}(t). \tag{4.13}$$

We used 64 points between every two consecutive integer values of t to calculate $D(t)$. As shown in Fig. 5, the deviation from linearity in the interval between any pair of J and $J-1$ appears to be very close to a parabola. To test this observation more rigorously, we fitted the data between each pair of $J-1$ and J to a set of second-order polynomials. Having obtained the analytical expressions for these polynomials, $D_{\mathrm{fit}}(t)$, we then solved the equation

$$\frac{\partial D_{\mathrm{fit}}(t)}{\partial t} = k, \tag{4.14}$$

where k is the slope of the function $E^{\mathrm{DFA}}_{\mathrm{linear}}(t)$ calculated between the same two integer values of t as those between which Eq. (4.14) is being solved. The solutions of

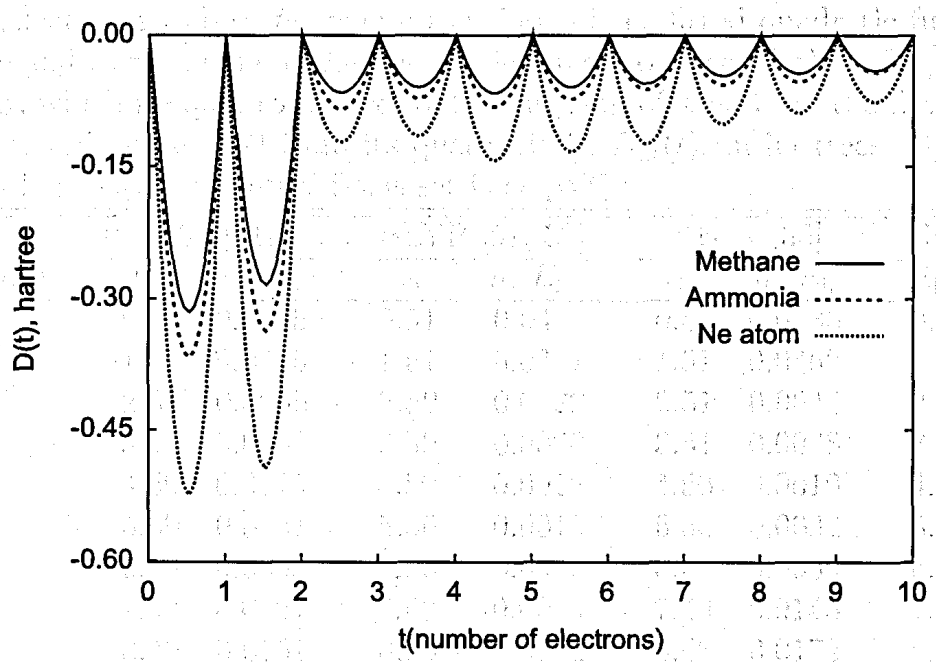

Fig. 5: Deviation from the linearity, $D(t)$, of the total energy as a function of the electron number calculated from an approximate density-functional approximation (exchange part of the PBE exchange-correlation functional).

Eq. (4.14) are such values of t, denoted by $t_{\rm lin}$, where $E^{\rm DFA}_{\rm actual}(t)$ would have the same slope as the $E^{\rm DFA}_{\rm linear}(t)$ if the deviation between these functions, $D(t)$, were exactly quadratic. In Table 4, we show the values $t_{\rm lin}$ calculated for the water molecule from various density-functional approximations. For the functionals studied, the fractional part of the values of $t_{\rm lin}$ is always very close to 1/2. This result supports our observation that $E^{\rm DFA}_{\rm actual}(t)$ is a piecewise-quadratic function. As an additional measure of the quadraticity, we also include in Table 4 the quantity σ defined by

$$\sigma = \left\{ \sum_i [D(t_i) - D_{\rm fit}(t_i)]^2 \right\}^{1/2} , \qquad (4.15)$$

where the summation is over all intermediate values from the range $J - 1 \leq t \leq J$ at which the function $D(t)$ was computed. On average, values of σ are of the order of ten millihartrees with higher values for the 1-, 2-, 8-, and 9-electron systems, and lower values for the 5-electron system. The lowest values of σ for the neutral 10-electron system indicate that the total energy is quite close to the quadratic function

Table 4: Electron numbers $t_{\rm lin}$ where the slope of the fitted quadratic function $D_{\rm fit}(t)$ becomes equal to the slope of the line connecting two integer values $E^{\rm DFA}_{\rm linear}(t)$, and the quantity σ, which is equal to square root of the sum of squares of the deviations of the actual observed curve $D(t)$ from its quadratic fit $D_{\rm fit}(t)$, in hartrees. System is H_2O molecule of the C_{2v} symmetry. Basis set is cc-pVQZ.

	B88 [51]		BLYP [51, 52]		PBEx [35]		PBExc [35]	
Range of t	$t_{\rm lin}$	σ, $E_{\rm h}$	$t_{\rm lin}$	σ, $E_{\rm h}$	$t_{\rm lin}$	σ, $E_{\rm h}$	$t_{\rm lin}$	σ, $E_{\rm h}$
0–1	0.51	0.0445	0.51	0.0445	0.51	0.0483	0.51	0.0485
1–2	1.51	0.0425	1.51	0.0327	1.51	0.0462	1.51	0.0451
2–3	2.51	0.0065	2.50	0.0029	2.51	0.0044	2.51	0.0048
3–4	3.51	0.0061	3.50	0.0020	3.51	0.0038	3.50	0.0035
4–5	4.50	0.0013	4.50	0.0012	4.50	0.0010	4.50	0.0008
5–6	5.50	0.0031	5.50	0.0010	5.50	0.0032	5.50	0.0026
6–7	6.50	0.0053	6.50	0.0012	6.50	0.0059	6.50	0.0038
7–8	7.49	0.0121	7.49	0.0085	7.49	0.0143	7.49	0.0153
8–9	8.49	0.0151	8.49	0.0102	8.48	0.0172	8.48	0.0154
9–10	9.50	0.0005	9.50	0.0001	9.50	0.0004	9.50	0.0003

in the range between 9 and 10 electrons. Since one often wants to calculate the ionization energy of a neutral system, the lowest values of σ for the neutral system will make the estimated ionization energy closer to the energy difference $E_{J-1} - E_J$. In Tables 5 and 6 we show the values of $t_{\rm lin}$ and σ for atoms H through Ar for the exchange functional of Perdew, Burke and Ernzerhof. The main message conveyed in these tables is that the more electrons there are in a system, the more quadratic the function $D(t)$ is.

As a side remark, note that the deviation from linearity is much higher for systems in the range $0 \leq t \leq 2$ electrons. This may be somehow related to the fact that the difference between the orbital- and subshell-aufbau paths is more pronounced in the same region, as discussed in Section 2.

As evident from Tables 4–6, the total energy calculated from the density-functional approximations studied here is close to piecewise-quadratic. For these functionals, the function $D(t)$ has a curtain-like shape shown in Fig. 5. This shape, together with the quadraticity, imply that the slope of a $(J - 1/2)$-electron system is equal to the slope of the straight line connecting the energy values of J and $(J - 1)$-electron systems.

Table 5: Values of t_{lin} calculated from the exchange part of the exchange-correlation functional of Perdew, Burke and Ernzerhof. The number of points between any two adjacent integers is 64. The basis set used is cc-pVQZ.

Range of t	H	He	Li	Be	B	C	N	O	F	Ne	Na	Mg	...	Ar
0–1	0.51	0.51	0.51	0.51	0.51	0.51	0.51	0.51	0.51	0.51	0.51	0.51		0.51
1–2		1.51	1.51	1.51	1.51	1.51	1.51	1.51	1.51	1.51	1.51	1.51		1.51
2–3			2.50	2.50	2.50	2.50	2.50	2.50	2.50	2.50	2.51	2.51		2.50
3–4				3.51	3.50	3.50	3.50	3.50	3.50	3.50	3.51	3.51		3.50
4–5					4.50	4.50	4.50	4.50	4.50	4.50	4.50	4.50		4.50
5–6						5.50	5.50	5.50	5.50	5.50	5.50	5.50		5.50
6–7							6.50	6.50	6.50	6.50	n/c	n/c		n/c
7–8								7.50	7.50	7.50	7.50	7.50		7.50
8–9									8.50	8.50	8.50	8.50		8.50
9–10										9.50	9.50	9.50		n/c
10–11											10.50	10.50		10.50
11–12												11.50		11.50
12–13														12.50
...														...
15–16														15.50
16–17														16.50
17–18														17.50

Table 6: Values of σ (in hartrees) calculated from the exchange part of the exchange-correlation functional of Perdew, Burke and Ernzerhof. The number of points between any two adjacent integers t is 64. The basis set used is cc-pVQZ.

Range of t	H	He	Li	Be	B	C	N	O	F	Ne	Na	Mg	...	Ar
0–1	0.0051	0.0112	0.0174	0.0236	0.0297	0.0359	0.0421	0.0483	0.0545	0.0607	0.0660	0.0722		0.1093
1–2		0.0087	0.0150	0.0213	0.0276	0.0338	0.0400	0.0462	0.0524	0.0587	0.0652	0.0714		0.1084
2–3			0.0008	0.0014	0.0019	0.0024	0.0029	0.0034	0.0039	0.0043	0.0057	0.0061		0.0090
3–4				0.0012	0.0018	0.0024	0.0029	0.0034	0.0039	0.0043	0.0056	0.0060		0.0090
4–5					0.0005	0.0003	0.0006	0.0011	0.0015	0.0019	0.0023	0.0028		0.0055
5–6						0.0004	0.0003	0.0007	0.0011	0.0015	0.0020	0.0025		0.0049
6–7							0.0004	0.0002	0.0005	0.0009	n/c	n/c		n/c
7–8								0.0003	0.0006	0.0011	0.0021	0.0023		0.0047
8–9									0.0003	0.0006	0.0015	0.0016		0.0041
9–10										0.0002	0.0004	0.0006		n/c
10–11											0.0003	0.0002		0.0005
11–12												0.0003		0.0005
12–13														0.0010
...														...
15–16														0.0008
16–17														0.0004
17–18														0.0002

Table 7: Ionization energies I_J calculated in three different ways: as the negative of the energy of the highest-occupied molecular orbital calculated from the $(J-1/2)$-electron system, from the J-electron system, and as the difference in total energies between the J- and $(J-1)$-electron systems. The basis set used is cc-pVQZ

		PBExf [35]			B88 [51]		
	Exact[a] $I(J)$	$-\epsilon_{\mathrm{HOMO}}(J-1/2)$	$-\epsilon_{\mathrm{HOMO}}(J)$	$[E(J-1)-E(J)]$	$-\epsilon_{\mathrm{HOMO}}(J-1/2)$	$-\epsilon_{\mathrm{HOMO}}(J)$	$[E(J-1)-E(J)]$
H	0.5000	0.5043	0.2700	0.4942	0.5068	0.2715	0.4978
He	0.9037	0.8828	0.5516	0.8642	0.8851	0.5528	0.8681
Li	0.1981	0.2003	0.1090	0.1986	0.1998	0.1091	0.1969
Be	0.3426	0.3021	0.1814	0.2993	0.3008	0.1811	0.2964
B	0.3050	0.2967	0.1360	0.2981	0.2971	0.1365	0.2982
Ne	0.7945	0.7501	0.4452	0.7498	0.7492	0.4456	0.7487
Na	0.1887	0.1904	0.1027	0.1909	0.1888	0.1026	0.1873
Al	0.2200	0.2021	0.0961	0.2022	0.2026	0.0967	0.2026
Ga	0.2205	0.1990	0.0919	0.1999	0.1994	0.0924	0.2001
Ar	0.5791	0.5351	0.3406	0.5348	0.5345	0.3402	0.5341
Kr	0.5145	0.4753	0.3052	0.4754	0.4752	0.3047	0.4752

[a]For atoms H through Al we use the difference in the non-relativistic total energies (Refs. [40, 41]) of the neutral atom and corresponding cation. For atoms Ga through Kr we use experimental estimates of the ionization energies available in Ref. [53].

As discussed above, the slope of the total energy is equal to the HOMO energy. Therefore, the energy of the HOMO calculated from the $(J-1/2)$-electron system is the best possible single-point estimate of the energy difference $(E_J - E_{J-1})$ and, consequently, is the best possible single-point estimate of the ionization energy I_J, at least for the functionals studied. To support this conclusion numerically, we ran a set of calculations on atoms. In Table 7, we compare the exact ionization energies to the ones estimated by the single-point calculations of the HOMO energy of the J- and $(J-1/2)$-electron systems. For the sake of completeness, we also include the two-point $(E_{J-1} - E_J)$ estimates of the ionization energy. The single-point estimates obtained from $(J-1/2)$-electron system, are always better than those computed from J-electron systems. Improvement is in the range from 30 to 50%. Generally, the $(J-1/2)$-ionization energies are slightly better (within the range of a few percent) than the two-point estimates. Nevertheless, there remain cases when single-point estimates are slightly worse than the two-point estimates.

Our experience shows that the quality of orbital energies is related to the quality of the approximate exchange-correlation potential used to generate them. We found that the quality of the HOMO is greatly improved if the orbitals are calculated from a $(J-1/2)$-electron system. In such systems, the HOMO energy can even become exact for some density-functional approximations. Altogether, this strongly suggests that the *exchange-correlation potential* calculated from a $(J-1/2)$-electron system is of a higher quality than the one calculated from the corresponding J-electron system. The use of half-electron-deficient potentials opens a new avenue in DFT. Therefore, if someone is to continue this project, exploration of various new possible ways of employing such potentials should receive the highest priority. The first thing to do would be to try using electron-deficient potentials in self-consistent calculations of the corresponding integer-electron systems.

References

[1] P. Hohenberg and W. Kohn, "Inhomogeneous electron gas," *Phys. Rev.* **136**, B864 (1964).

[2] M. Levy, "Universal variational functionals of electron densities, first-order density matrices, and natural spin-orbitals and solution of the v-representability problem," *Proc. Nat. Acad. Sci. USA* **76**, 6062 (1979).

[3] R. van Leeuwen, "Density-functional approach to the many-body problem: key concepts and exact functionals," *Adv. Quantum Chem.* **43**, 25 (2003).

[4] W. Kohn and L. J. Sham, "Self-consistent equations including exchange and correlation effects," *Phys. Rev.* **140**, A1133 (1965).

[5] R. G. Parr and W. Yang, *Density-Functional Theory of Atoms and Molecules.* Oxford University Press: New York, 1989.

[6] S. P. Sousa, P. A. Fernandes, and M. J. Ramos, "General performance of density functionals," *J. Phys. Chem. A* **111**, 10439 (2007).

[7] R. van Leeuwen and E. J. Baerends, "Exchange-correlation potential with correct asymptotic behavior," *Phys. Rev. A* **49**, 2421 (1994).

[8] O. Gritsenko, R. van Leeuwen, E. van Lenthe, and E. J. Baerends, "Self-consistent approximation to the Kohn–Sham exchange potential," *Phys. Rev. A* **51**, 1944 (1994).

[9] A. Lembarki, F. Rogemond, and H. Chermette, "Gradient-corrected exchange potential with the correct asymptotic behavior and the corresponding exchange-energy functional obtained from the virial theorem," *Phys. Rev. A* **52**, 3704 (1995).

[10] O. V. Gritsenko, R. van Leeuwen, and E. J. Baerends, "Structure of the optimized effective Kohn–Sham exchange potential and its gradient approximations," *Int. J. Quantum Chem.* **57**, 17 (1996).

[11] O. V. Gritsenko, R. van Leeuwen, and E. J. Baerends, "Direct approximation of the long- and short-range components of the exchange-correlation Kohn–Sham potential," *Int. J. Quantum Chem.* **61**, 231 (1997).

[12] O. V. Gritsenko, P. R. T. Schipper, and E. J. Baerends, "Approximation of the exchange-correlation Kohn–Sham potential with a statistical average of different orbital model potentials," *Chem. Phys. Lett.* **302**, 199 (1999).

[13] M. Grüning, O. V. Gritsenko, and E. J. Baerends, "Shape corrections to exchange-correlation potentials by gradient-regulated seamless connection of model potentials for inner and outer region," *J. Chem. Phys.* **114**, 652 (2001).

[14] V. Karasiev, E. V. Ludeña, and R. López-Boada, "SCF calculations with density-dependent local-exchange potential," *Int. J. Quantum Chem.* **70**, 691 (1998).

[15] V. Karasiev and E. V. Ludeña, "Asymptotically adjusted self-consistent multiplicative parameter exchange-energy-functional method: Application to diatomic molecules," *Phys. Rev. A* **65**, 032515 (2002).

[16] M. E. Casida and D. R. Salahub, "Asymptotic correction approach to improving approximate exchange-correlation potentials: Time-dependent density-functional theory calculations of molecular excitation spectra," *J. Chem. Phys.* **113**, 8918 (2000).

[17] M. K. Harbola and K. D. Sen, "Improved Becke88 and PW91 exchange potentials," *J. Phys. B* **35**, 4711 (2002).

[18] N. Umezawa, "Explicit density-functional exchange potential with correct asymptotic behavior," *Phys. Rev. A* **74**, 032505 (2006).

[19] A. D. Becke and E. R. Johnson, "A simple effective potential for exchange," *J. Chem. Phys.* **124**, 222101 (2006).

[20] V. N. Staroverov, "A family of model Kohn–Sham potentials for exact exchange," *J. Chem. Phys.* **129**, 134103 (2008).

[21] E. Räsänen, S. Pittalis, and C. R. Proetto, "Universal correction for the Becke–Johnson exchange potential," *J. Chem. Phys.* **132**, 044112 (2010).

[22] S. Pittalis, E. Räsänen, and C. R. Proetto, "Becke–Johnson-type exchange potential for two-dimensional systems," *Phys. Rev. B* **81**, 115108 (2010).

[23] R. van Leeuwen and E. J. Baerends, "Energy expressions in density-functional theory using line integrals," *Phys. Rev. A* **51**, 170 (1995).

[24] V. Volterra in: *Theory of Functionals and of Integral and Integro-Differential Equations*, L. Fantappiè, ed., p. 226. Blackie: London, Glasgow, 1930.

[25] S. Liu and R. G. Parr, "Expansions of the correlation-energy density functional $E_c[\rho]$ and its kinetic-energy component $T_c[\rho]$ in terms of homogeneous functionals," *Phys. Rev. A* **53**, 2211 (1996).

[26] A. P. Gaiduk, S. K. Chulkov, and V. N. Staroverov, "Reconstruction of density functionals from Kohn–Sham potentials by integration along density scaling paths," *J. Chem. Theory Comput.* **5**, 699 (2009).

[27] A. P. Gaiduk and V. N. Staroverov, "How to tell when a model Kohn–Sham potential is not a functional derivative," *J. Chem. Phys.* **131**, 044107 (2009).

[28] M. Levy in: *Density Functional Theory*, E. K. U. Gross and R. M. Dreizler, eds., pp. 11–31. Plenum: New York, 1995.

[29] J. P. Perdew, L. A. Constantin, E. Sagvolden, and K. Burke, "Relevance of slowly varying gas to atoms, molecules, and solids," *Phys. Rev. Lett.* **97**, 223002 (2006).

[30] T. Ziegler and A. Rauk, "On the calculation of bonding energies by the Hartree–Fock–Slater method," *Theor. Chim. Acta* **46**, 1 (1977).

[31] H. Ou-Yang and M. Levy, "Theorem for exact local exchange potential," *Phys. Rev. Lett.* **65**, 1036 (1990).

[32] M. Levy and J. P. Perdew, "Hellmann–Feynman, virial, and scaling requisites for the exact universal density functionals. Shape of the correlation potential and diamagnetic susceptibility for atoms," *Phys. Rev. A* **32**, 2010 (1985).

[33] S. K. Ghosh and R. G. Parr, "Density-determined orthonormal orbital approach to atomic energy functionals," *J. Chem. Phys.* **82**, 3307 (1985).

[34] P. M. W. Gill, "A new gradient-corrected exchange functional," *Mol. Phys.* **89**, 433 (1996).

[35] J. P. Perdew, K. Burke, and M. Ernzerhof, "Generalized gradient approximation made simple," *Phys. Rev. Lett.* **77**, 3865 (1996).

[36] J. C. Slater, "A simplification of the Hartree–Fock method," *Phys. Rev.* **81**, 385 (1951).

[37] M. J. Frisch, G. W. Trucks, H. B. Schlegel, G. E. Scuseria, M. A. Robb, J. R. Cheeseman, J. A. Montgomery, Jr., T. Vreven, G. Scalmani, B. Mennucci, V. Barone, G. A. Petersson, M. Caricato, H. Nakatsuji, M. Hada, M. Ehara, K. Toyota, R. Fukuda, J. Hasegawa, M. Ishida, T. Nakajima, Y. Honda, O. Kitao, H. Nakai, X. Li, H. P. Hratchian, J. E. Peralta, A. F. Izmaylov, K. N. Kudin, J. J. Heyd, E. Brothers, V. Staroverov, G. Zheng, R. Kobayashi, J. Normand, J. L. Sonnenberg, S. S. Iyengar, J. Tomasi, M. Cossi, N. Rega, J. C. Burant, J. M. Millam, M. Klene, J. E. Knox, J. B. Cross, V. Bakken, C. Adamo, J. Jaramillo, R. Gomperts, R. E. Stratmann, O. Yazyev, A. J. Austin, R. Cammi, C. Pomelli, J. W. Ochterski, P. Y. Ayala, K. Morokuma, G. A. Voth, P. Salvador, J. J. Dannenberg, V. G. Zakrzewski, S. Dapprich, A. D. Daniels, M. C. Strain, O. Farkas, D. K. Malick, A. D. Rabuck, K. Raghavachari, J. B. Foresman, J. V. Ortiz, Q. Cui, A. G. Baboul, S. Clifford, J. Cioslowski, B. B. Stefanov, G. Liu, A. Liashenko, P. Piskorz, I. Komaromi, R. L. Martin, D. J. Fox, T. Keith, M. A. Al-Laham, C. Y. Peng, A. Nanayakkara, M. Challacombe, W. Chen, M. W. Wong, and J. A. Pople, *Gaussian Development Version, Revision F.02.* Gaussian, Inc.: Wallingford CT, 2006.

[38] H. Engels, *Numerical Quadrature and Cubature.* Academic Press: London, Toronto, 1980.

[39] P. J. Davis and P. Rabinowitz, *Methods of Numerical Integration.* Academic Press: Orlando, Toronto, 2nd ed., 1984.

[40] E. R. Davidson, S. A. Hagstrom, S. J. Chakravorty, V. M. Umar, and C. Froese Fischer, "Ground-state correlation energies for two- and ten-electron atomc ions," *Phys. Rev. A* **44**, 7071 (1991).

[41] S. J. Chakravorty, S. R. Gwaltney, E. R. Davidson, F. A. Parpia, and C. Froese Fischer, "Ground-state correlation energies for atomic ions with 3 to 18 electrons," *Phys. Rev. A* **47**, 3649 (1993).

[42] E. Engel and S. H. Vosko, "Accurate optimized-potential-model solutions for spherical spin-polarized atoms: Evidence for limitations of the exchange-only local spin-density and generalized-gradient approximations," *Phys. Rev. A* **47**, 2800 (1993).

[43] J. F. Janak, "Proof that $\partial E/\partial n_i = \epsilon_i$ in density-functional theory," *Phys. Rev. B* **18**, 7165 (1978).

[44] M. M. Valiev and G. W. Fernando *Phys. Rev. B* **52**, 10697 (1995).

[45] J. C. Slater, *Quantum Theory of Molecules and Solids*, vol. 4. McGraw-Hill: New-York, 1974.

[46] J. P. Perdew, "What do the Kohn–Sham orbitals mean? How do atoms dissociate?," in: *Density Functional Methods in Physics*, R. M. Dreizler and J. da Providencia, eds., pp. 265–308. Plenum Press: New York and London, 1985.

[47] I. Dabo, A. Ferretti, N. Poilvert, Y. Li, N. Marzari, and M. Cococcioni, "Koopmans condition for density-functional theory," *Phys. Rev. B* **82**, 115121 (2010).

[48] J. P. Perdew, R. G. Parr, M. Levy, and J. L. Balduz, "Density-functional theory for fractional particle number: derivative discontinuities of the energy," *Phys. Rev. Lett.* **49**, 1691 (1982).

[49] J. C. Slater and J. H. Wood, "Statistical exchange and the total energy of a crystal," *Int. J. Quantum Chem.* **4S**, 3 (1971).

[50] J. C. Slater, "Statistical exchange-correlation in the self-consistent field," *Adv. Quantum Chem.* **6**, 1 (1972).

[51] A. D. Becke, "Density-functional exchange-energy approximation with correct asymptotic behavior," *Phys. Rev. A* **38**, 3098 (1988).

[52] C. Lee, W. Yang, and R. G. Parr, "Development of the Colle–Salvetti correlation-energy formula into a functional of the electron density," *Phys. Rev B* **37**, 785 (1988).

[53] D. R. Lide, ed., *Handook of Chemistry and Physics.* CRC Press: Boca Raton, 72 ed., 1992.

A Description of auprog program

Capabilities

Auprog is a program for calculating exchange-correlation energies via the van Leeuwen–Baerends line integral formula [Eq. (2.5)]. The supported density parametrization include the Λ-path for exchange-only potentials with the energy expression from Eq. (2.12), the Q-path, and the orbital- and subshell-aufbau paths.

The supported density-functional approximations include the integrable exchange potentials of Gill, and of Perdew, Burke and Ernzerhof. For these potentials, auprog can calculate the energies via the corresponding parent functionals $E_{\mathrm{x}}^{\mathrm{G96}}$ and $E_{\mathrm{x}}^{\mathrm{PBE}}$. Among the non-integrable potentials, the exchange potentials of Umezawa, and of van Leeuwen and Baerends are available.

The supported technique for the integration over the density parametrizing parameter (q or t) is the Gauss–Legendre quadrature. The number of nodes can be chosen during runtime, and is within the range of 1 to 1000 per pair of consecutive integer values of the scaling parameter.

Interface

Auprog is invoked from the command line in the Linux environment. It accepts up to four command-line arguments. The first argument is the name of the configuration file. The second is the file containing the electron density and other ingredients that are obtained from an external program (GAUSSIAN in our case). The third argument is the name of the file to which the intermediate data is written. This data is used, for example, for generating figures like Fig. 2. The fourth argument is the name of a file containing the Fermi–Amaldi potential computed on a grid. The Fermi–Amaldi potential is an ingredient of the Umezawa potential, so the fourth auprog's argument is meaningful only when calculations with the Umezawa potential are requested, and

is ignored otherwise. `Auprog` writes its output to the Linux standard output.

The configuration file for `auprog` consists of lines formatted in the following way

```
A B C DDD E GG HH II JJ K
```

Here all the letters represent integer numbers that are used to set the following configuration parameters:

`A` — Density-functional approximation to be used:
- `1` — Gill potential/functional
- `2` — Leeuwen–Baerends potential
- `3` — Perdew–Burke–Ernzerhof exchange potential/functional
- `4` — Umezawa potential

`B` — Way of computing the exchange energy
- `1` — functional (if applicable)
- `2` — line integration of a potential: Λ-path (Levy–Perdew formula)
- `3` — line integration of a potential: Q- and aufbau paths

`C` — Quadrature used for Q- and aufbau paths:
- `1` — Gauss–Legendre

Next parameters are meaningful only when calculations with Q- or aufbau paths are requested, i.e., when `B=3`.

`DDD` — Number of nodes in a quadrature

`E` — Density to be used:
- `1` — α spin-density
- `2` — β spin-density
- `3` — total density

`GG` — Number of fully occupied α spin-orbitals

`HH` — Number of α spin-orbitals with fractional occupations

`II` — Number of fully occupied β spin-orbitals

`JJ` — Number of β spin-orbitals with fractional occupations

`K` — Flag to control output of the value of the cumulative integral:
- `0` — requests further accumulation of cumulative integral
- `1` — requests printing of cumulative integral and then zeroes its value. New accumulation of (partial) aufbau-path energies starts at the first line with `B=3` and is continued up to a line with `K=1`.

The format of the configuration file is strict in the sense that if, for example, one wants to set a value of 32 to the parameter DDD, then one has to type 032.

As an example, consider the following configuration

```
4 3 1 256 1 00 01 00 00 0
```

This requests calculations with the Umezawa potential. The energy will be calculated using the van Leeuwen–Baerends line integral formula with density parametrized by the orbital-aufbau path. The integration over the parameter t will be done by a 256-node Gauss–Legendre quadrature. The value of cumulative integral is accumulated and can be requested by the next line in the configuration file. The above example generates the following output for the hydrogen atom:

```
##########   iLine  1:
Config: 4 3 1 256 1  0  1  0  0 0
Method:  Umz06    Way: Aufbau    Density:   A
--Quadrature: GauLeg  Nodes: 256
-----FullMOA: 0 SprMOA: 1 AvailMOA: 1
-----FullMOB: 0 SprMOB: 0 AvailMOB: 0
E=     -0.4853290905058887
I=     -0.4853290905058887
```

Here E is the exchange energy of interest, and I is the value of the cumulative integral. In this case they coincide because the hydrogen atom has only one electron.

Structure of auprog

Auprog is written in FORTRAN-95 and consists of more than 1200 lines of code. As a way to facilitate calculations, it uses the OpenMP multi-threading technique. The program depends on the GNU extensions of the FORTRAN language available in the gcc collection of compilers, and on the open-source open-access implementation of the Gauss–Legendre quadrature. The calling graph of auprog is shown on Fig. 6.

The Main program reads the configuration file into memory (RdConf). It also reads (RdIntg) integer parameters from the input file containing Kohn–Sham orbitals

and their derivatives. These parameters are then used in `Stage0`, where the dynamic allocation of memory is performed and where the rest of the data is read. Also, in `Stage0` the program sequentially performs calculations specified in every line of the configuration file. Depending on the calculation type requested, `auprog` branches to either `DFTs` or `Auf0`. If a calculation is single-point, i.e., if it involves no integration over the parameter t as it is for the Λ-path and for calculations via functionals, then the program executes `DFTs`. If the calculation requires integration over t, i.e., if the aufbau- or Q-path calculations are requested, then `auprog` executes the `Auf0` subroutine first. `Auf0` generates a quadrature grid (`GnQuad`, `ChIntv`, `GauLeg`) and then, at each gridpoint, also calls `DFTs`. The role of `DFTs` is to calculate an energy from the density built (`MO2Auf`) from partially- or fully- filled Kohn–Sham orbitals. It does that via `G09`, `PBE96x`, `Umz06`, `VLB94` subroutines depending on the method and the way requested.

Subroutines `PltPreamble`, `PrtRes` and `PlotPr` are responsible for `auprog`'s output. Subroutines `MkRhTot` and `RdFAPot`, respectively, construct the total electron density and read the Fermi–Amaldi potential needed for the calculations with the Umezawa potential. The subroutine `Int824` converts a 8-bit integer to the 4-bit integer, `ArrClr` is a subroutine that zeroes a given array, and `ASinH` calculates the inverse of the hyperbolic cosine function, which is present in the van Leeuwen–Baerends potential.

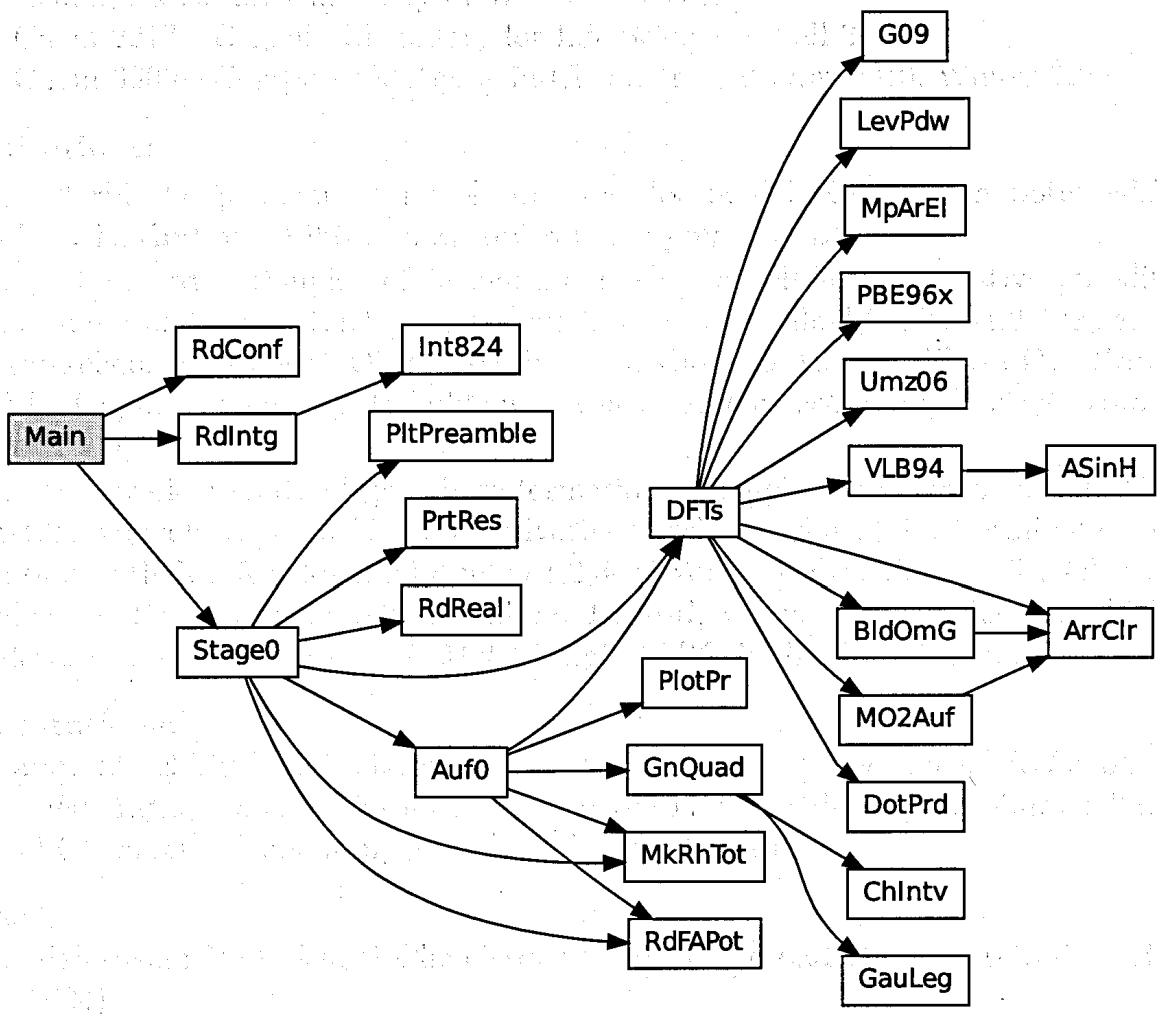

Fig. 6: Calling graph for auprog